The synthesis of large interstellar molecules

Eric Herbst

Published online: 10 Apr 2017.

Submit your article to this journal ⟲

View related articles ⟲

View Crossmark data ⟲

Taylor & Francis
Taylor & Francis Group

The synthesis of large interstellar molecules

Eric Herbst

Departments of Chemistry and Astronomy, University of Virginia, Charlottesville, VA, USA

ABSTRACT

This review is concerned with the formation of molecules in the interstellar medium (ISM), which is composed mainly of regions of gas and dust known as interstellar clouds, ranging in size from a few to 100's of light years in extent. Upwards of 200 different molecules have been observed spectroscopically in these objects, with a significant fraction of them 'large' by astronomical standards; i.e. containing six or more atoms. Interstellar clouds are of interest to chemists because of the exotic molecules and chemistry that occur in these sources, while they are of interest to astronomers because these clouds are the only known birthplaces of new stars and extrasolar planets. The formation of stars and planets from portions of dense interstellar clouds is a complex evolutionary process with multiple stages dependent upon the mass of the collapsing object. For low-mass stars such as our sun, the process is reasonably well understood and proceeds through the following intermediate stages: cold dense cores, pre-stellar cores, hot cores, and protoplanetary discs. For high-mass stars, the process is significantly less well understood because these objects are rare and are formed through evolutionary stages that are short in duration, at least astronomically speaking. Molecules are found in all of these stages, in the gas phase and often in the solid phase, with the chemistry dependent upon the physical conditions and their history. Indeed, the many molecules detected have helped significantly to unravel much of the complexity involved in stellar and planetary formation. This review is divided into sections in which, following an introduction, we discuss the different types of chemical reactions that synthesise large molecules, starting with cold dense cores of temperature 10 K and gas density 10^{10} m^{-3}, and proceeding through the various stages of low-mass star formation through protoplanetary discs. Several other types of sources are discussed briefly. We then review some recent progress that has occurred within the last several years in improving our knowledge of the chemistry in this fast-growing and rapidly evolving field of research. We end with a brief discussion of the detailed chemical simulations employed to follow the chemistry in the various sources in the ISM.

Contents

1. Introduction

The earth is but a small portion of the universe, which is replete with molecules. Indeed, the phrase 'the molecular universe' has been utilised in a previous review article [1]. This present review, designed principally for physical chemists, contains a long discussion of what was known about the chemistry and synthesis of large interstellar molecules up to several years ago, and then adds to this a discussion of the significant amount of recent

work done since that time. We start with a basic introduction to astronomy, especially the interstellar medium (ISM), and the molecules found in assorted interstellar sources.

The universe consists principally of galaxies, which come in a variety of shapes and sizes. The visible matter in galaxies is mainly composed of stars, which are hot and bright, and dominate the visible portion of the spectrum. But, in addition to stars, about 10% of the matter in galaxies is interstellar in origin. The so-called ISM is not homogeneous, but is concentrated into regions of relatively dense gas and tiny dust particles known as interstellar clouds, with the dust-to-gas ratio 0.01 by mass and $\approx 3 \times 10^{-12}$ by number. The largest interstellar clouds can have a size of up to several hundred pc (1 pc = 3.1×10^{16} m = 3.28 lt yr), and are known as 'giants.' Although clouds are themselves inhomogeneous, they are often classified as 'diffuse', 'translucent', and 'dense'. Diffuse clouds have gas densities in the range $n \approx 10^7 - 10^8 \, \mathrm{m}^{-3}$ and kinetic temperatures in the range 50–100 K, where the term 'kinetic' temperature refers to the kinetic energy of translation. These clouds can generally transmit enough radiation in the visible region of the spectrum to allow spectra of gas-phase atoms and molecules to be detected in optical absorption with background stars as the light sources. Dust particles cause most of the weak diminution of light. Although the gas is mainly atomic, some small molecules have been detected in the gas, and one large one – C_{60}^+. A large number of diffuse bands remain unidentified, and may be spectra of other large molecules. The major small molecule formed is molecular hydrogen, which can only be produced efficiently under interstellar conditions by association of two hydrogen atoms on the surfaces of dust particles. Although astronomers use optical depth τ, they often prefer to use a logarithmic historical term known as visual extinction and labelled by A_V, where five units of extinction refer to a factor of 100 diminution. For diffuse clouds, a typical visual extinction is about unity, meaning that a diminution of $100^{1/5}$ = 2.51 occurs as external visual radiation passes through the cloud. The scattering and absorption of light through diffuse clouds as a function of wavelength yields information on the size distribution of dust particles, which lie between 1 nm and 0.3 μm with the smaller particles more abundant than the larger ones [2,3].

Unlike diffuse clouds, dense clouds possess too much matter for visible radiation to penetrate ($A_V \geq 10$), again caused mainly by continuous scattering and absorption of background radiation by dust particles [3]. Spectroscopy can be performed to study dense clouds at longer wavelengths than the visible, specifically from the infrared to the radio, where the extinction decreases with increasing wavelength. Dense interstellar clouds are of great interest in astronomy because they are the only known sources of stars and planets, which are formed when cold cores in the clouds collapse and eventually heat up [4]. Such clouds can appear dark, due to the inability of visible light to penetrate them, or bright, if stars have already formed. Clouds with many stars born within them are often referred to as 'giant.' Dense clouds are of interest to chemists because the gas is overwhelmingly molecular in nature, with many exotic species detected and exotic kinetic processes deduced to explain their abundances. Molecules and their spectra are excellent probes of the physical conditions of clouds.

Dense clouds are heterogeneous, with the densest ($n \approx 10^{10} \, \mathrm{m}^{-3}$) and coldest (10 K) regions known as 'cold cores.' Because stars are continuous emitters in the infrared but not usually at longer wavelengths, infrared spectroscopy can be performed in absorption against a stellar background and used to detect gas phase molecules and the molecular constituents of ice mantles surrounding cold dust particles. Based on spectroscopic studies,

the dust particles can be divided into two classes - metallic silicates and amorphous carbon – depending upon the type of star that produces them and ejects them into the ISM. The silicates can be detected based on infrared spectral features, whereas the amorphous carbon, or other forms of carbon, can be detected in the ultra-violet in diffuse clouds [3]. Infrared astronomy is a difficult technique using ground-based telescopes, because atmospheric water vapor, even above deserts, blocks out much radiation in this region. Space telescopes are expensive to use as spectrometers, but a number of infrared space telescopes have been launched and one will be launched in the near future. A high-altitude airplane observatory also exists. Infrared techniques have been used to identify molecular vibrations of only a few ice constituents in the mantles of cold dust, including water, the dominant species, CO_2, CO, CH_3OH, CH_4, NH_3, and possibly NCO^- [3]. The standard technique to identify gaseous molecules is to study their rotational spectra which, up to quite high frequencies, can be done from the ground [4]. Exceptions include non-polar molecules, e.g. H_3^+, and two neutral fullerenes C_{60} and C_{70}, which have been detected in the infrared [5,6]. The fullerene cation C_{60}^+ has been identified in electronic absorption towards four diffuse clouds via five spectral lines in the near-infrared [7]. Almost ubiquitous but unidentified aromatic features seen in emission have been assigned to a large number of polycyclic aromatic hydrocarbons (PAH's) [8,9].

   Rotational spectra are normally seen in emission, and are excited by collisions with other molecules or, in active star-forming regions, with radiation [4]. A detailed analysis of the collisional excitation can yield the overall gas density as well as the so-called rotational temperature. In addition, the Doppler shift can yield the macroscopic motion of the source being studied, including collapse, expansion, and rotation [10]. The gaseous molecular inventory determined mainly by rotational spectroscopy without differentiating among the different types of interstellar sources includes almost 200 molecules, not counting isotopomers, with up to twelve atoms in size. Molecules with six or more atoms are known, somewhat surprisingly, as 'complex organic molecules.' Here we have replaced the word 'complex' with 'large.' Both chemical processes and elemental abundances help to determine the molecules formed. Elemental abundances are best determined in stellar atmospheres such as the sun. In interstellar clouds, the abundances that pertain to the gas plus ice mantles are depleted by the material making up the cores of dust particles. In addition, different sets of gaseous abundances are best for dense and diffuse clouds, and are often referred to as 'high metal' (for diffuse clouds) and 'low metal' (for dense clouds) where the word 'metal' refers in a non-chemical sense to elements heavier than helium. Table 1 contains a selected list of the major 'low metal' elemental abundances with respect to the total number of protons, a term that refers to the sum of the atomic hydrogen abundance added to twice the molecular hydrogen abundance [11,12]. These numbers also refer to the initial form (ionic, atomic, molecular) used by modellers in calculating the abundances of molecules as function of time in cold dense cores, but really pertain to diffuse clouds since there is no obvious criterion for the initial abundances in a cold core. The atomic positive ions are used for all elements with an ionisation potential less than hydrogen, because these neutral atoms are ionised by collisions and radiation. Photons of energy greater than 13.6 eV would be needed to ionise hydrogen; such radiation is normally weak to non-existent because the photons are absorbed by hydrogen in stellar atmospheres and do not reach the ISM. Given the high elemental abundances of C, N, and O, Table 1 shows clearly why organic chemistry dominates the list of interstellar molecules.

Table 1. 'Low-Metal' elemental abundances for interstellar clouds and initial forms of elements.[a]

Element/Form	Value with respect to total hydrogen nuclei
H_2	5.00×10^{-1}
He	9.00×10^{-2}
N	2.14×10^{-5}
O	1.76×10^{-4}
e^-	7.31×10^{-5}
C^+	7.30×10^{-5}
S^+	8.00×10^{-8}
Si^+	8.00×10^{-9}
Fe^+	3.00×10^{-9}
Na^+	2.00×10^{-9}
Mg^+	7.00×10^{-9}

[a] See Acharyya and Herbst [12] for more detail.

An up-to-date listing of interstellar species can be found in assorted web pages; see, for example http://www.astrochymist.org/ or https://www.astro.uni-koeln.de/cdms/. The most abundant molecule is molecular hydrogen, which is not surprising given that hydrogen is the most abundant element in most of the universe. The second most abundant species is CO, which has a fractional abundance with respect to H_2 of 10^{-4}. The abundances and classes of larger species depend strongly on physical conditions although most are organic in nature. For cold cores, the molecular inventory includes hydrogen-poor radicals, positive and negative molecular ions, surprisingly abundant isomers, and very unsaturated linear 'carbon chains' consisting of long chains of carbon atoms with at least one more atom to make the molecule polar [4]. These are usually referred to as 'exotic', and certainly are exotic when compared with terrestrial organic chemistry, whereas warmer sources involved in the evolutionary path to stars show a chemistry that is much more terrestrial in nature. In these warm sources, commonly known as 'hot cores', the molecules detected in the gas include esters, ethers, alcohols, and nitriles [4]. The distinction between the two types of cores is not completely clear cut; terrestrial type molecules exist to a small extent in cold cores, and some exotic species exist in hot cores. The unsaturated species seen especially in cold cores indicate that the elemental abundances, which are dominated by hydrogen, do not explain why there is so little hydrogen in these species; obviously, a rather unusual chemistry is occurring. It should also be mentioned that the sulfur elemental abundance is not well constrained, with some dense regions possessing a much higher abundance than shown in Table 1 [13].

The first and so far only chiral molecule detected in the gas phase is propylene oxide (CH_3CHOCH_2) [14], which has been detected in rotational absorption against a warm region near the center of our galaxy. Although enantiomeric excesses have possibly been found in meteorites [15], determining the abundance ratio of the two enantiomers of propylene oxide is likely to be very difficult. One suggestion is a photochemistry that can distinguish among enantiomers based on circularly polarised light [16]; this is likely to be an improvement on circular dichroism, which is a very small effect. Beta decay related chemical processes can also generate small chiral asymmetries [17].

1.1. *The Stellar-cloud cycle: star formation and destruction*

The synthetic chemistry of classes of interstellar molecules will be discussed in terms of the evolutionary stages of low-mass star formation, so a brief introduction to this topic is necessary [18]. Figure 1 shows some of the stages in the formation of low-mass stars like the sun as well as high-mass stars. It must be realised that astronomers cannot view the evolutionary process in all its dynamic glory since the time scales are too large. Much of our information is found by observing individual stages as static objects and inferring their order in the scheme of things. The evolution of low-mass stars is much the better understood, both because there are many more of them, including some quite close to the earth, and because their stages take longer periods of time. The low-mass case appears to be at least somewhat cyclic in that it begins and ends with a star and possibly planets orbiting it. Although this view is an oversimplification, it is useful to think in terms of this cycle.

We start with an old star, which appears on the left central portion of the figure. Old low-mass stars eject dust and gaseous matter into the diffuse ISM, which eventually collapses under the influence of gravity to form dense interstellar clouds, containing denser and dark portions known as cold cores. There is an intermediate physical structure between diffuse and dense clouds; this structure is called a translucent cloud, and has a density of 10^8 – 10^9 m^{-3} and a visual extinction of $\approx$3. It takes cold cores 10^{5-6} yr for the chemistry to form the exotic unsaturated molecules already discussed. A fraction of cold cores are known to collapse; the objects are then called pre-stellar cores. The initial collapse is isothermal in nature; the temperature remains constant, unlike the prediction of the virial theorem, because the object is still optically thin in some regions of the electromagnetic spectrum. Eventually, a dense condensation forms in the middle of the collapsing core, and the collapse turns adiabatic due to its optical thickness. The condensation heats up and begins to form a young star, a stage known as a protostar. We then use the term 'low-mass young stellar object' to refer to the protostar and the collapsing material.

As material collapses inward towards the condensation, it heats up. When a temperature of 100–300 K is reached by the collapsing gas, we refer to the material, the gas phase of which is dominated by terrestrial organic species, as a 'hot core', or, if it is of low-mass, the term 'hot corino' is sometimes used. At the same time, in the presence of angular momentum, a protoplanetary disc begins to form perpendicular to the angular momentum vector and material is blown out of the protostar in a dipolar flow with associated shocks. The gas-phase chemistry of protoplanetary disks is much less rich than that of cold cores or hot corinos because, with the exception of material quite close to the budding star, the high density of cold dust particles allows gas-phase species to accrete rapidly so that it is difficult to detect them in the gas phase. Meanwhile, the dust particles coalesce into larger objects, eventually forming comets, meteors, and even planets. The star settles down on the main sequence, with a core that burns protons into helium ions, and eventually reaches old age.

The situation regarding high-mass stars is somewhat different, and it is unclear if protoplanetary discs ever form around young high-mass stars. In place of cold core condensations, there are higher-mass condensations known as infrared dark clouds, which contain a number of dense cores of somewhat higher temperature. These cold objects show a similar chemistry to low-mass cold cores and eventually collapse through several stages, including a hot core, to form clusters of high-mass stars, which light up and ionise the material surrounding them. The ionised material is known as an HII region. Bright high-
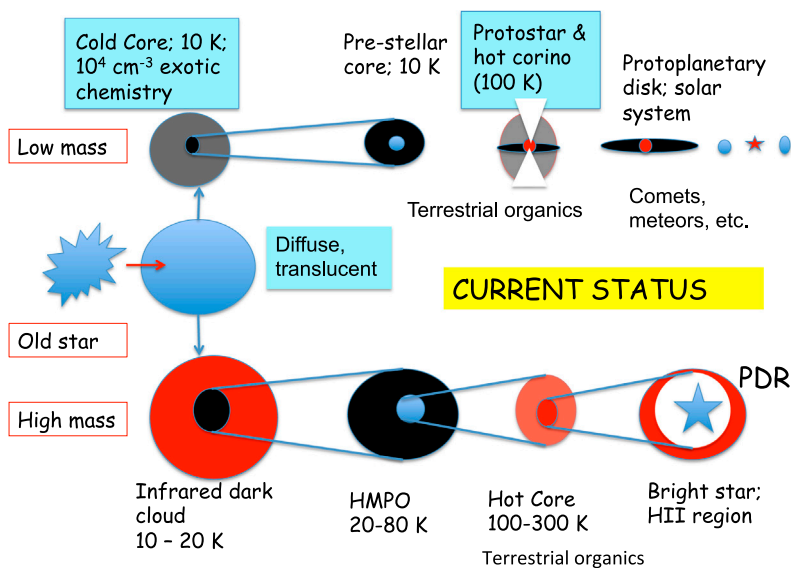
Figure 1. Stages of low-mass and high-mass star formation. The acronym HMPO stands for 'high-mass protostellar object.' See assorted chapters in Lis et al. [18]. Based on the author's figure for a power point presentation.

mass stars can then affect the chemistry of nearby material, which is referred to as a photon-dominated region (pdr). The hot cores formed during high-mass star formation share the terrestrial-type chemistry of hot corinos, but are much warmer and more luminous. Shocks and PDR's will be discussed later in Section 3.3.

2. Classes of reactions and their role in cold molecular synthesis

Cold cores, and to a lesser extent, infrared dark clouds, are known for the synthesis of exotic and strongly unsaturated organic molecules at temperatures as low as 10 K. Table 2 lists all of these molecules with six or more atoms detected in interstellar sources and some circumstellar sources, especially around older stars. The table contains positive and negative molecular ions (e.g. HC_2CNH^+ and C_6H^-), unusual isomers (e.g. H_2CCCC), unsaturated radicals (e.g. $C_{2n}H$; $n = 3, 3.5, 4$), and polar carbon chains known as cyanoolyynes ($HC_{2n}CN$; $n = 2, 3, 4, 5$). Not all are associated with cold sources; E-cyanomethanimine (E–HNCHCN) has only been detected towards the hot core source Sagittarius B2(N), while HC_4H (1,3 – buta-di-yne) and HC_6H (1,3,5 – hexa-tri-yne) which are non-polar, were detected in the infrared in the circumstellar source surrounding a carbon star named IRC 10216. A more complete list of the gas-phase reactions discussed below in the synthesis of the molecules in Table 2 can be found either in the databases http://udfa.ajmarkwick. net/ or http://kida.obs.u-bordeaux1.fr/ along with many other synthetic and destruction reactions as well. References are also provided for those reactions studied in the laboratory or theoretically. The KIDA database is discussed in a paper by Wakelam et al. [19]. It should be noted that although many of the more important reactions discussed here have been studied to some extent, many others have not, especially at low temperatures.

Table 2. 'Large' exotic and unsaturated species in the interstellar and circumstellar media.[a]

6-atomic	7- atomic	8-atomic	9-atomic	$\geq$10-atomic
C_5N	C_6H	C_7H	C_8H	HC_8CN
C_5N^-	C_6H^-	$H_2CCCCCC$	C_8H^-	$HC_{10}CN$
C_5H	HC_4CN	HC_6H	HC_6CN	
HC_4N				
H_2CCCC				
HC_2CNH^+				
HC_4H				
$c\text{-}H_2C_3O$				
$E\text{--}HNCHCN$				

[a]Criteria: (1) linear and near linear; (2) at most two H atoms. Exotic molecules with fewer than six atoms can be found in http://www.astrochymist.org/.

A partial explanation of the formation of these unusual molecules derives from gas phase ion-neutral chemistry. These reactions have been well studied in the laboratory over a wide temperature range, and often obey simple long-range theories as long as they are exothermic and have channels without activation energy barriers [20]. Reactions between ions and non-polar neutrals often occur with the temperature-independent Langevin rate constant k_L, which is easily derived by using a capture hypothesis with a simple long range $-1/r^4$ potential between the charge of the ion and the polarisability of the neutral. In SI units, the equation for the Langevin rate constant is

$$k_L = \sqrt{\frac{\pi \alpha' q^2}{\epsilon_0 \mu}},\qquad(1)$$

where α' is the polarisability volume (m^3), q is the elementary charge (C), and μ (kg) is the reduced mass of the reactants. The major non-polar neutral reactant in interstellar sources is molecular hydrogen,and the dominant reaction between an ion X^+ and H_2 is H-atom transfer to form $XH^+ + H$. For this reaction and the ion O^+, the calculated Langevin rate constant is 1.57×10^{-15} m^3 s^{-1}, while the measured value at 300 K is 1.62×10^{-15} m^3 s^{-1} [21]. A large tabulation of measured ion-neutral rate constants with an emphasis on astrochemical usage has been provided by Anicich [21].

Ion-polar neutral reactions cannot be treated as simply since the long-range potential also depends upon the angle between the reactant ion and the rotating dipole moment of the neutral. Nevertheless, approximate treatments exist, and can be found in the literature [20,22–24]. The rate constant goes as $T^{-1/2}$ at low temperatures until a quantum limit is reached at approx. 5 K, but gradually, as temperature rises, the temperature dependence lessens until the temperature-independent Langevin relation is reached. Low temperature ion-polar rate constants can reach values as high as $\approx 10^{-13}$ m^3 s^{-1}. A new treatment by Ervin [25] shows additional effects beyond the existence of a permanent dipole, in particular those due to the quadrupole moment, and the polarisability of the ion.

The production of neutrals via ion-neutral reactions often proceeds via some number of hydrogenation reactions normally involving H-atom transfer from H_2 up to a maximum number of hydrogens m, which can represent a fully saturated ion or just a species which does not react appreciably with H_2. For example, consider the following sequence of

reactions starting from bare X^+:

$$X^+ \rightarrow XH^+ \rightarrow XH_2^+ \rightarrow \cdots \rightarrow XH_m^+. \tag{2}$$
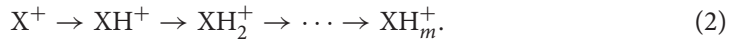
Once the maximum number of H atoms is reached, the positive ion XH_m^+ then can undergo dissociative recombination with electrons:

$$XH_m^+ + e^- \longrightarrow XH_{m-1} + H, XH_{m-2} + 2H, \text{etc.} \tag{3}$$
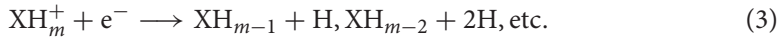
Dissociative recombination reactions have large rate constants of $\approx 10^{-12} \, \text{m}^3 \, \text{s}^{-1}$ to $\approx 10^{-13} \, \text{m}^3 \, \text{s}^{-1}$ at room temperature with an inverse temperature dependence of $T^{-1/2}$ [20,26] but the fractional abundance of electrons in dense cold sources is calculated to be $\approx 1 \times 10^{-7}$ with respect to total hydrogen, so that reactions with H_2, if they occur with the Langevin rate constant, are much faster. Recent studies using magnetic storage rings and position sensitive detectors have delineated the product channels and found that three-body channels tend to be much stronger than two-body channels in most cases unless the three-body channels are endothermic [26]. An example is the reaction between $H_3O^+ + e^-$, in which $OH + 2H$ is the dominant product channel [27,28]. This tendency of dissociative recombination reactions is one reason why unsaturated species are so prevalent in cold cores.

2.1. Details of ion-neutral synthetic pathways

In order to power an ion-neutral chemistry at low temperatures, there must be some non-thermal source of ionisation. Although there are local sources of ionisation, such as X-rays and UV photons, the latter especially in diffuse clouds, the global source of ionisation consists of cosmic rays, which are mainly high-energy nuclei, especially protons, formed in supernova explosions and accelerated to near the speed of light. Although cosmic rays cause ionisation and also produce local ultra-violet radiation, their penetrating power is very high. A low-energy cosmic ray of 6 MeV can ionise $\approx 10^5$ molecules. The flux of cosmic rays is not uniform in space, and this flux decreases as the cosmic rays traverse a dense cloud [29,30]. Moreover, the low energy cosmic rays, which possess the largest cross section for ionisation, are difficult to measure near the earth because of the solar wind. Nevertheless, a first-order rate constant for cosmic-ray ionisation of H_2 is typically assumed to be $\approx 10^{-17} \, \text{s}^{-1}$ inside a cold core, while it may be as much as two orders of magnitude larger in diffuse clouds and on the edges of dense clouds [31].

The dominant cosmic ray ionisation product channel for H_2 is the production of electrons and H_2^+ [32]; the H_2^+ ion then quickly (within a day) reacts with another H_2 to produce H_3^+ via the well-studied reaction [21]:

$$H_2^+ + H_2 \longrightarrow H_3^+ + H. \tag{4}$$

The triangular ion H_3^+ does not react with H_2 and is abundant enough to play the major role in the onset of molecular synthesis. Another important ion in the synthesis of larger species is C^+, which is the dominant ion in diffuse clouds, with a fractional abundance of 10^{-4}. Its abundance gradually decreases in dense clouds as C^+ is slowly and partially converted to neutral C, which is subsequently mainly consumed in the formation of CO.

Some C^+ is maintained by the reaction of CO and He^+ [21]. Eventually, the abundance of C^+ becomes somewhat less than that of H_3^+ and HCO^+, which have fractional abundances of $\approx 5 \times 10^{-9}$ in cold cores, approximately 0.1 that of electrons, the dominant negative charge carrier.

Let us see how H_3^+, C, and C^+ start an organic chemistry that leads to the unusual species detected in cold cores [33]. First, C and C^+ are 'fixed' into ionic hydrocarbons via the reactions

$$C + H_3^+ \longrightarrow CH^+ + H_2; CH_2^+ + H, \tag{5}$$
$$C^+ + H_2 \longrightarrow CH_2^+ + h\nu. \tag{6}$$
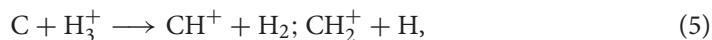
The first process is a standard H-atom transfer with another mechanism to form CH_2^+ [34], while the second process is an example of a radiative association, which can be of importance at low densities, where ternary association is inefficient [20]. It plays a significant role in carbon fixation because the more standard H-atom transfer to CH^+ + H is quite endothermic and therefore slow at 10 K. Radiative association is itself an exotic process, and can be thought of as proceeding via a temporary complex, which either dissociates or can be stabilised by emission of a photon, normally from vibrational relaxation in the ground electronic state, but occasionally via relaxation from an excited electronic state. Although experiments with ion trap techniques have been used to measure low-density binary association reactions, assumed to be radiative in nature, the detection of emitted photons has, to the best of our knowledge, not been successful [35,36]. According to statistical theories [20,37], radiative association is most efficient when the complex is long-lived, which becomes more likely when one or more of the following criteria are met: (1) a low temperature, (2) a large (multi-atom) complex, and (3) a large potential well depth. A simple thermal theory for polyatomic complexes shows that as long as the collisional value of the rate constant has not been reached, the dependence on temperature goes as $T^{-(r_A+r_B+1)/2}$, where r_A and r_B are the number of rotational degrees of freedom of the reactants, as long as rotation can be treated continuously [38]. So, for two non-linear tops, $r = 3$ and the overall inverse temperature dependence is $T^{-3.5}$. For C^+ + H_2, on the other hand, the inverse temperature dependence is predicted to be only $T^{-1.5}$, and this prediction may be too large for the 10–100 K range since rotation may need to be treated discretely. The actual measured value for the reaction at 25 K is $\approx 5 \times 10^{-22}$ $m^3 s^{-1}$, in reasonable agreement with modified thermal and phase space theories [39]. Despite its low rate constant, it is competitive with recombination of C^+ and electrons, which is much slower than dissociative recombination.

The CH_2^+ ion can be formed by reaction (5) [34] or via the H-atom transfer reaction between CH^+ and H_2. The CH_2^+ ion can be hydrogenated only up to CH_3^+ by H-atom transfer reactions because the methyl ion does not react rapidly with H_2 in this manner. On the other hand, the radiative association with H_2 has been studied in the laboratory and is reasonably efficient at low temperatures, with $k \approx 10^{-19}$ $m^3 s^{-1}$ at 13 K [36]. Despite the low value of this rate constant, the overall rate is competitive with dissociative recombination because the reactant H_2 is the most abundant neutral species by four orders of magnitude. The dissociative recombination of CH_5^+ produces mainly the methyl radical and small species, and it turns out that methane is produced mainly by the reaction of the

protonated ion with CO:

$$CH_5^+ + CO \longrightarrow CH_4 + HCO^+. \tag{7}$$

Carbon monoxide is formed by a multitude of reactions, one of which is the dissociative recombination of HCO^+ with electrons. Other formation processes include reactions between various neutral hydrocarbon radicals and atomic oxygen.

There are several synthetic approaches for forming large species in cold cores. We will limit the discussion initially to the growth of unsaturated hydrocarbons. One approach is based on reactions between C^+ and neutral hydrocarbons [21]; e.g.

$$C^+ + CH_4 \longrightarrow C_2H_3^+ + H; C_2H_2^+ + 2H. \tag{8}$$
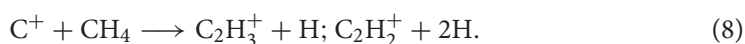
Note that in addition to adding a carbon atom to methane, the process removes 1-2 hydrogen atoms. The ions produced can then react with H_2 by H-atom transfer if exothermic and barrierless, or by radiative association. The most hydrogenated ion produced in this manner is $C_2H_4^+$, which then undergoes dissociative recombination to form acetylene among other hydrocarbons. Acetylene reacts with C^+ to form $C_3H^+ + H$, with subsequent hydrogenation leading only to $C_3H_2^+$ and $C_3H_3^+$. Both the cylic and non-cyclic forms of C_3H_2 can then be produced by dissociative recombination of cyclic and non-cyclic precursor ions [40]. In general, it is thought without much evidence that dissociative recombination cannot produce a variety of isomeric forms, unless the skeletal structure of the precursor ion remains unchanged. On the other hand, experimental evidence that dissociative recombination can lead to isomeric products with a common heavy atom structure exists for the ion $HCNH^+$, where it leads to both HNC and HCN [41]. This precursor ion can be formed by the reaction between C^+ and NH_3, where ammonia is itself formed via a sequence of hydrogenation reactions that lead to NH_4^+ [21].

A similar but less well studied sequence leading to the formation of unsaturated hydrocarbons consists of reactions between neutral atomic carbon and hydrocarbon ions. Somewhat more saturated hydrocarbon ions and neutrals are produced by condensation reactions, in which a hydrocarbon ion and a hydrocarbon neutral react with one another to form a larger hydrocarbon and hydrogen [21]; e.g.

$$C_2H_2^+ + CH_4 \longrightarrow C_3H_5^+ + H \tag{9}$$
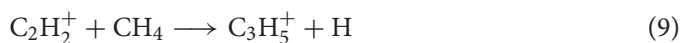
followed by dissociative recombination. Such reactions are less efficient than the C^+ and C pathways, but can lead to more saturated neutral hydrocarbons such as CH_3CCH. In general, due to both the increasing difficulty in hydrogenating hydrocarbon ions as the number of carbon atoms in the hydrocarbon skeleton increases as well as dissociative recombination, the number of hydrogen atoms in the molecules decreases with increasing carbon number until hydrocarbons with 1-2 hydrogen atoms only are produced efficiently; e.g. the C_nH and HC_nH families and their carbene isomers. These general ideas have been extended to the formation of unsaturated cyclic hydrocarbons through fullerenes, but not PAH's. In this synthesis, closely based on laboratory syntheses, linear chain unsaturated hydrocarbons grow until they convert spontaneously to single ring species. Further growth leads to tri-cyclic species and finally to fullerenes [42].

In addition to the two linear hydrocarbon families discussed in the above paragraph, ion-neutral pathways can also lead to the cyanopolyyne family (HC_2CN, HC_4CN, HC_6CN, HC_8CN). The major reactions are thought to involve the nitrogen atom and non-cyclic hydrocarbon ions, viz.:

$$N + C_nH_3^+ \longrightarrow H_2C_nN^+ + H, \tag{10}$$
$$N + C_nH_4^+ \longrightarrow H_3C_nN^+ + H, \tag{11}$$
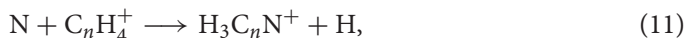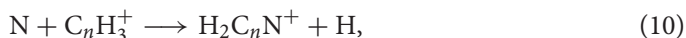
followed by dissociative recombination although experimental evidence is only available for the production of protonated HC_2CN [21]. Here n is an odd number starting with $n = 3$. Radiative association reactions involving polyatomic ions and neutrals can account at least partially for some more saturated nitrogen-containing molecules such as CH_3CN and CH_3NC, which are formed by the association between CH_3^+ and HCN followed by dissociative recombination [43]. Ion-neutral reactions also lead to exotic unsaturated oxygen-containing molecules, but these are not 'large' and so are not discussed here [44].

Not all large molecules found in cold cores are exotic and/or very unsaturated. Four important exceptions are methanol (CH_3OH), acetaldehyde (CH_3CHO), dimethyl ether (CH_3OCH_3) and methyl formate ($HCOOCH_3$). For some time, it was thought that the radiative association between CH_3^+ and H_2O to produce $CH_3OH_2^+$ followed by dissociative recombination leads to methanol in cold sources. Indeed, the association reaction does occur as a three-body process at high densities. However, the predicted value of the radiative association rate constant is much larger than the experimental value, which is actually only an upper limit [45]. In addition, the dissociative recombination of protonated methanol produces little or no methanol, so that the methanol observed in cold cores cannot be produced in this manner at sufficient abundance [46]. Nor can it be produced efficiently by any other gas-phase process. Its production occurs on dust particle surfaces, as discussed below. The three other molecules can be formed in the gas via neutral–neutral chemistry or on dust particles, as also discussed in subsequent sections.

2.1.1. Isotopic fractionation

Ion-neutral reactions play an important role in what is known as isotopic fractionation, in which the abundance ratio of an isotopologue to the normal species is different from the ratio of the elemental abundances. The largest effect is observed with deuterium. For example, in sea water on earth the HDO/H_2O abundance ratio is 1.5×10^{-4} whereas the D/H elemental abundance ratio is 10^{-5} throughout much of the nearby universe. In cold interstellar clouds, the deuterated isotopologue can be enhanced for many minor species by orders of magnitude. The major source of deuterium in dense interstellar clouds is HD, which is not strongly fractionated. In the ISM, the fractionation is mainly chemical in nature and at low temperature involves the abundant ion H_3^+. Consider the forward and reverse ion-neutral reactions between H_3^+ and HD:

$$H_3^+ + HD \rightleftarrows H_2D^+ + H_2. \tag{12}$$

The left-to-right process is exothermic by $\approx 232\,K$, where we have used the astronomical sign convention as well as dividing the enthalpy by the Boltzmann constant [47]. At temperatures under 20 K, the equilibrium lies strongly to the right, and the H_2D^+/H_3^+

abundance ratio in cold cores can reach a rather large value at low temperatures, which is calculated to be greater than 10^7 [47]. But a simple equilibrium is not reached because the destruction of H_2D^+ occurs not by the back reaction with H_2, but by reactions with CO (to produce DCO^+ and HCO^+), electrons, and HD (to produce D_2H^+). The resulting abundance ratio at 10 K is calculated to be $\approx 0.1 - 0.2$ [48]. This range of values is still much larger than 10^{-5}, but not easy to measure since the deuterated species has a dipole moment with a resultant rotational spectrum while the normal species must be detected in the infrared. It is far easier to measure the abundance ratio DCO^+/HCO^+, which is determined to be $\approx 0.02 - 0.06$, since both species have rotational transitions in convenient regions of the spectrum [49]. Theoretical values are also in this range in reasonable agreement with observation [48]. In the centre of pre-stellar cores, the density of gas and dust is much greater due to collapse, and there is little CO left in the gas because it accretes onto the grains. The result is an even higher abundance ratio of H_2D^+/H_3^+, which can exceed unity, in agreement with theory [50]. In fact, in one source, the H_2D^+ ion is found to be the most abundant ion towards the centre. Moreover, the D_2H^+ ion has also been detected in pre-stellar cores. A prediction that the most abundant ion should be D_3^+ cannot be confirmed because the vibrational transition has not yet been observed, an observation that cannot be undertaken from the ground [50]. Once there are high abundances of selected deuterated species, ion-neutral reactions can spread the deuterium to more complex species. Detailed discussions of how the primary deuterated species spread the deuteration fractionation throughout other species in cold regions are given in a number of early references [33,48,50–52].

It should be mentioned, however, that all of these predictions assume that H_2 lies mainly in its ground (para) $J = 0$ rotational state at low temperatures. The existence of a substantial population in the excited $J = 1$ ortho state allows the backward endothermic reaction in reaction (12) to occur more rapidly since it is less endothermic and to thereby reduce the calculated fractionation. This possibility is likely to happen only at early times when the H_2 has yet to come close to its thermal rotational distribution, a time-consuming process that occurs via reactions with protons. Recent simulations including deuterium fractionation with ortho/para effects have been reported [53–55]. Other ions that can extend the deuterium fractionation to higher temperatures due to greater exothermicity in reactions with HD include CH_3^+, with an exothermicity of 370 K and $C_2H_2^+$, with an exothermicity of 550 K, to produce CH_2D^+ and C_2HD^+, respectively [56].

The fractionation of $^{13}C/^{12}C$ is far less dramatic but can be used to deduce the reaction chains that form specific organic species by the strength of the fractionation and, if two different isotopomers are formed, by their relative abundances; viz. ^{13}CCH and $C^{13}CH$. By the first method, the formation route of methanol is found to start from CO rather than C^+ [57], while by the second method, the formation routes of CCH and CCS can be identified [58]. Nitrogen fractionation has also been a subject of interest [59].

2.1.2. Negative ions

We now come to the problem of the formation of negative ions. The abundances of negative ions, when expressed as ratios to the respective neutrals, are largest for molecular families with high electron affinities such as the C_nH family. Moreover, the abundance ratio of the anion to the neutral is largest for the largest ions detected. For example, the abundance ratios of C_2H^-/C_2H, C_4H^-/C_4H, C_6H^-/C_6H, C_8H^-/C_8H in the cold core TMC-1 are

observed to be <0.00033, <0.000052, 0.016, and 0.046, respectively [60]. In another core, L1527, the C_4H^-/C_4H abundance ratio has been measured to be 0.00011 although the ratio C_2H^-/C_2H is still only an upper limit of 0.000036 [60]. Although the abundances of anions and their neutrals are obtained by rather complex simulations involving both formation and destruction processes [61,62], the strong dependence of the anion/neutral abundance on size suggests that a radiative association is involved, known here as radiative attachment; viz.,

$$C_nH + e^- \longrightarrow C_nH^- + h\nu, \tag{13}$$
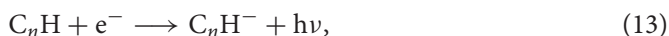
in which a negatively charged complex is stabilised by emission of a photon [63]. Once primary negative ions are formed in this manner, ion-neutral reactions can produce secondary ions. Use of a statistical theory, in which the attachment rate constant increases with increasing size of the reactant, has proven controversial, however, as some but not all detailed scattering theory calculations indicate no such size dependence is to be expected [64,65]. The rate of radiative relaxation has also been controversial, since it can involve simply vibrational deexcitation, or electronic relaxation from a dipole-bound electronic state. Other mechanisms have been suggested such as reactions involving H^- as the primary ion [66], and exothermic dissociative attachment between high energy isomeric species and electrons; viz.,

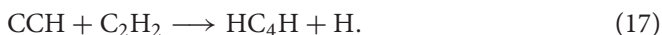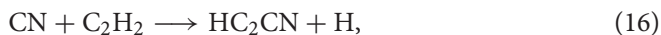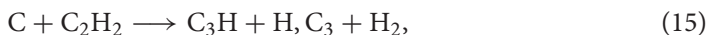$$H_2C_6 + e^- \longrightarrow C_6H^- + H, \tag{14}$$

which would be highly endothermic if the lower energy HC_6H isomer were used [67].

Condensation reactions involving negative ions and neutral hydrocarbons have been implicated in the production of very large organic molecules in the atmosphere of the carbon-rich star IRC+10216, and to a lesser extent in the cold core TMC-1 [61,68].

2.2. Contribution of neutral–neutral reactions

Ion-neutral/dissociative recombination pathways towards complexity in cold cores are supplemented by neutral–neutral reactions. Originally considered only in a minor way in the models of the 1970s and 1980s, neutral–neutral reactions began to take on a more important role when it was realised that selected reactions between normal neutral species and radicals can proceed without activation energy and even increase in rate constant to a limit of about $10^{-16}\,m^3\,s^{-1}$ at a temperature in the vicinity of 10 K. The major experimental technique used in the study of low-temperature neutral–neutral reactions, first devised by Bertran Rowe et al., is the Lavalle nozzle technique, most frequently known by the French acronym CRESU, which stands for *Reaction Kinetics in a Uniform Supersonic Flow* [69]. Up to the present, it has been difficult to measure products with this technique, and other approaches such as the merged beam and crossed beam techniques have been used to obtain products when there is more than one exothermic channel, albeit mainly at higher temperatures. As examples of well-studied systems, three important reactions in the chemistry of cold dense clouds involve acetylene and the atoms/radicals C, CN, C_2H:

$$C + C_2H_2 \longrightarrow C_3H + H, C_3 + H_2, \tag{15}$$
$$CN + C_2H_2 \longrightarrow HC_2CN + H, \tag{16}$$
$$CCH + C_2H_2 \longrightarrow HC_4H + H. \tag{17}$$

These reactions have been studied down to temperatures of 15, 25, and 15 K, respectively [70–72]. Other analogous reactions involving larger hydrocarbons provide competitive formation pathways to ion-neutral reactions for large unsaturated hydrocarbons and cyanopolyynes.

Neutral reactions in the cold gas can involve species that are formed on grains and then desorbed into the gas. A most important reaction of this type is the formation of acetaldehyde from the gas phase reactants O and C_2H_5:

$$O + C_2H_5 \longrightarrow CH_3CHO + H. \tag{18}$$
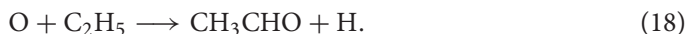
The C_2H_5 radical is not formed appreciably in the gas, but is formed by hydrogenation on cold grains and then desorbed non-thermally, as discussed in Section 4.5. Acetaldehyde is found in cold cores despite the fact that it is not a carbon chain but a terrestrial organic species. There are a few other such molecules that are found in the gas phase of cold cores, albeit at abundances much lower than they possess in hot cores. These species include methanol, methyl formate ($HCOOCH_3$) and dimethyl ether (CH_3OCH_3). The formation of these species is discussed in Sections 4.1 and 4.2 under recent advances.

Although radiative association reactions between neutral species have not been included except for a few isolated cases in networks for chemical simulations of interstellar sources, such processes are thought to occur in the upper atmosphere of the Saturnian moon Titan, which has an atmosphere full of organic molecules [73].

2.3. Contribution of dust particle reactions

The chemistry that can occur on dust particle mimetics, especially on ice mantle surfaces, has seen much experimental interest in the last decade, after it was realised that not all molecular abundances in the ISM could be explained by gas-phase chemistry [74]. In cold regions, the dust chemistry involves physisorption, which, unlike chemisorption, can involve a large number of monolayers. In cold cores, the number of monolayers of ice, formed both by accretion from the gas and from chemical reactions on and in the ice, can exceed 100 after 10^6 yr. Although the chemistry that occurs on bare silicate and carbonaceous dust surfaces, before ice mantles develop, can be regarded as surface chemistry, the study of chemistry as ice mantles develop is more accurately described as ice chemistry, which can occur both on surfaces and within the ice. For simulations in which both gas-phase and ice/grain chemistry are included, the two must be connected by accretion and desorption mechanisms. Sticking probabilities at low temperatures are near unity so that accretion volume rates are given simply by the product of the granular density, the density of the accreting species, the granular cross section, the speed of the gas-phase species, and another factor to take into account the geometry of the grain. With 100% sticking, the accretion rate for atomic hydrogen per grain, with a gas-phase abundance of $1.0 \times 10^6 \, m^{-3}$, and a spherical grain of radius $0.1 \, \mu m$ at 10 K is $\approx 10^{-5} \, s^{-1}$.

There are two types of desorption: thermal and non-thermal [75]. Thermal desorption is normally thought to be a first-order process with a rate constant k_{TD} given by the relation

$$k_{TD}(T) = \nu_0 \exp{(-E_D/kT)}, \tag{19}$$

where ν_0, known as the 'attempt' frequency, is typically $\approx 1 - 3 \times 10^{12}\,\mathrm{s}^{-1}$ for light physisorbed species, and E_D is the minimum energy needed for desorption [33,76]. Even for physisorbed species, the desorption energies are large enough except for H, H_2, and He that thermal desorption does not occur in cold cores, but only in warmer sources involved with star formation. Non-thermal mechanisms operative at low temperatures include intact photodesorption, reactive desorption, cosmic ray desorption, and photodissociative desorption, which are discussed in Section 4.5.

There are three major mechanisms for reaction on surfaces; these are known as the Langmuir–Hinshelwood (LH), Eley–Rideal (ER), and hot atom mechanisms. Figure 2 illustrates the first two of these. The LH mechanism involves thermal diffusion of two surface species until they find each other and react whereas the ER mechanism involves a near head-on collision between a gas-phase species and an adsorbate. The hot atom mechanism bears some similarity to both the LH and ER processes; here the species that lands on the surface can travel with some extra, non-thermal energy to find an adsorbate and react with it. One specific example in interstellar clouds occurs when a cosmic ray particle strikes a grain and, among other effects, globally heats the grain to a distribution of temperatures in the range 30–100 K [77]. The higher temperature raises the rate of diffusion. In this section, we restrict attention mainly to the thermal diffusive mechanism, since it is the best understood of the three and is used in most simulations of interstellar dust chemistry. One major difference between gas-phase and dust chemistry is that association reactions play a stronger role in the latter, because grains act as if they are third bodies in ternary association reactions, allowing the dissipation of energy to stabilise the reaction product.

For a surface diffusive reaction between species A and B without activation energy, the rate of reaction can be approximated by the equation [33,78]

$$\frac{d\theta(A)}{dt} = -(k_{\mathrm{hop,A}} + k_{\mathrm{hop,B}})\theta(A)\theta(B), \qquad (20)$$

where θ refers to the number of monolayers of a species, which can be a fractional value, and k_{hop}, the first-order rate constant for hopping, pertains to the rate over or through a diffusive barrier from one binding site to a neighbouring binding site. Note that hopping refers to climbing over one barrier between surface binding sites, whereas the term diffusion refers normally to the possibility of randomly moving over many sites by single hops. Better approximations exist at the expense of an increase in complexity [79]. The formula for this rate constant depends upon whether classical hopping or quantum mechanical tunnelling prevails. In the case in which hopping dominates, the formula is [20,33,76]

$$k_{\mathrm{hop}} = \nu_0 \exp{(-E_b/kT)}, \qquad (21)$$

where ν_0 is once again the attempt frequency, which is typically $1 - 3 \times 10^{12}\,\mathrm{s}^{-1}$ for physisorption, and E_b is the barrier between adjacent binding sites. For most reactions, one of the reactants moves much more quickly than the other, and so only one hopping or tunnelling rate is needed. The barrier is only spatially homogeneous for a simple crystal system, and can be highly variable for a so-called 'rough' surface, in which case a more complicated treatment of the kinetics, such as a kinetic Monte Carlo approach, is required. In the case of tunnelling, the simplest formula used is based on a rectangular barrier of
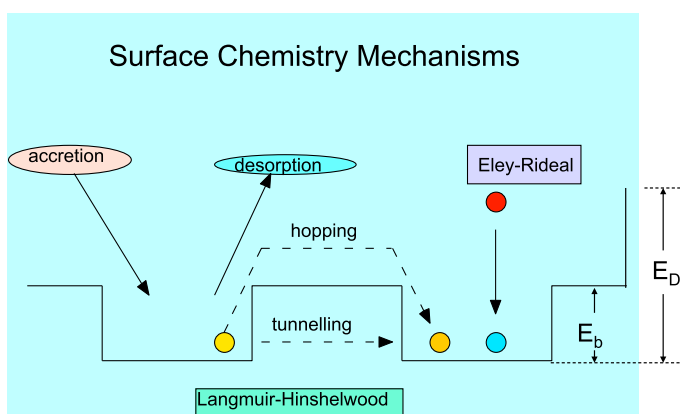
$$E_b = xE_D; \quad x = 0.3 - 0.8$$

Figure 2. Two of the three major surface reaction mechanisms. Based on the author's figure for a power point presentation. See text for the definitions of E_D and E_b.

width a [76]. For reactions with chemical activation energy E_A, an additional Boltzmann factor $\kappa = \exp(-E_A/kT)$ has often been used.

This formula for the diffusive rate of reaction is most accurate for systems in which fractions of a monolayer are present for both reactants, as almost always occurs for chemisorption. If more than a monolayer is present, and the chemistry is constrained to occur only on the top monolayer, the equation should refer only to this monolayer with the abundances of species in the lower monolayers constant in time. If chemistry can occur under the top monolayer, the particular mechanism will not be a simple diffusion; one alternate possibility is exchange (swapping) between two species [80]. Astrochemists distinguish between two types of treatments of ice chemistry [80,81]. The first is referred to as a two-phase model, in which the two phases are the gas phase and the mantle + surface phase. Here there is no distinction made between the surface and the internal ice layers; all species are treated in an identical manner as regards bimolecular collisions, although processes such as photodesorption and photodissociation are normally treated with a depth effect. The second treatment is known as a three-phase model, in which the three phases are the gas, the surface of the dust mantle, and the internal layers of the dust mantle. These are discussed in more detail in Section 5.

For physisorption, barriers between adjacent binding sites for adsorbates, E_b, which are difficult to measure, are normally approximated as fractions x of the total adsorbate binding energy against desorption, E_D, which can be measured by a number of techniques. The factor x has been estimated to be any number in the range 0.3–0.8 [82]. The lower the number the more rapid the diffusion and therefore the reaction. In cold cores, the diffusive chemistry on bare grains and ice mantles involves very weakly bound reactants, since only these can diffuse appreciably at 10 K. The most weakly bound species are mainly atoms and small molecules; of these, atomic hydrogen is the most weakly bound and the most likely to tunnel under barriers against diffusion as well as hopping over them. The evidence for tunnelling under diffusive barriers, however, is ambiguous at best, although
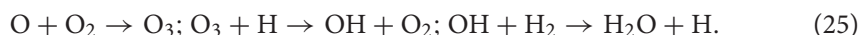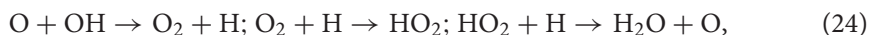
it has been claimed for oxygen atoms on very cold surfaces [83]. Despite the fact that most of the hydrogen is converted from its atomic to its molecular form on grains by the time of the young cold core stage, there is a residual abundance of atomic hydrogen, typically 10^{-4} of the molecular form. The atomic hydrogen is quite reactive on surfaces, even at 10 K, and can react with other hydrogen atoms to form H_2 as well as reacting with other neutral species [84]. The synthesis of methanol is an example of a mechanism that utilises atomic hydrogen; methanol is the largest molecule seen via infrared absorption to exist in the ice mantles of dust in cold regions.

The most detailed experimental studies to date of low temperature surface/ice processes concern the formation of molecular hydrogen, water, and methanol; in favourable cases, the experimental results can be converted into rate constants for the analogous reactions under interstellar conditions. In the case of molecular hydrogen, there is no efficient synthesis in the gas phase since radiative association between two hydrogen atoms has been found to have a vanishingly small rate constant [85]. Ion-neutral syntheses do exist at high temperatures, such as the process that involves the hydrogen anion:

$$H^- + H \longrightarrow H_2 + e^-, \tag{22}$$

but these are mainly relevant in the early universe [86]. The production of H_2 from two atoms on grains can occur via a variety of different mechanisms depending upon temperature and surface. At low temperatures, experiments show that the atoms are bound weakly by physisorption [87], while at higher temperatures, calculations indicate that chemisorption plays a major role [88].

The synthesis of water on cold and icy surfaces takes place via a variety of sequences of reactions involving H atoms, as well as O atoms, O_2 molecules, and even O_3 molecules [89]. For example, the following sequences of surface reactions lead to water ice:

$$O + H \rightarrow OH; OH + H \rightarrow H_2O, \tag{23}$$

$$O + OH \rightarrow O_2 + H; O_2 + H \rightarrow HO_2; HO_2 + H \rightarrow H_2O + O, \tag{24}$$

$$O + O_2 \rightarrow O_3; O_3 + H \rightarrow OH + O_2; OH + H_2 \rightarrow H_2O + H. \tag{25}$$

The simplest sequence, starting from O and H, is similar to sequences of reactions that produce surface NH_3 and CH_4.

From the point of view of complex molecule formation, the surface formation of methanol is exceedingly important, since methanol is a precursor of more complex species. As first postulated [90] and then confirmed [91,92] in the laboratory, this synthesis starts from CO, which is produced copiously in the gas and then accretes onto dust particles. Four surface reactions with atomic H convert the CO into formaldehyde and subsequently methanol:

$$CO + H \rightarrow HCO; HCO + H \rightarrow H_2CO; H_2CO + H \rightarrow H_3CO; H_3CO + H \rightarrow CH_3OH. \tag{26}$$
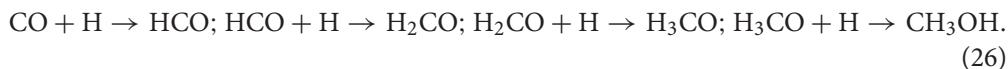
In addition to the production of the intermediate methoxy radical, its isomer, hydroxymethane (CH_2OH) is also formed [92]. The reactions to form HCO and CH_3O/CH_2OH have activation energy barriers of 10–20 kJ/mol. Although barriers such as these have often been treated by Boltzmann factors κ in the rate equations (see above), a more

Table 3. Terrestrial-type complex organic species in the interstellar medium.[a,b]

6-atomic & 7- atomic	8-atomic & 9-atomic	$\geq$10-atomic
CH_3OH^*	$HC(O)OCH_3^*$	$(CH_3)_2CO$
CH_3SH	$CH_3C(O)OH$	$(CH_2OH)_2$
CH_3CN^*	CH_2OHCHO	CH_3CH_2CHO
CH_3NC^*	CH_3CHNH	CH_3CHCH_2O
NH_2CHO^*	$(NH_2)_2CO$	$HC(O)OC_2H_5$
CH_2CHOH	NH_2CH_2CN	$CH_3OC(O)CH_3$
$c-C_2H_4O$	CH_2CHCH_3	$c-C_6H_6$
CH_3NCO	CH_3CH_2CN	$n-C_3H_7CN$
CH_3CHO^*	$(CH_3)_2O^*$	$i-C_3H_7CN$
	CH_3CH_2OH	$C_2H_5OCH_3$ (?)
	$CH_3C(O)NH_2$	
	CH_3CH_2SH (?)	

[a] Criteria: (1) at least 6 atoms; (2) at least four hydrogen atoms except for 6-atomic species.
[b] Most species found only in hot cores/corinos; some are also observed in cold cores or translucent clouds. These are listed with asterisks. Uncertain or disputed detections shown with question marks.

detailed treatment, which is becoming popular, treats the competition between activation energy and diffusive barriers. If the diffusive barriers are the larger, the reactants get many chances to hop over or tunnel under the activation barrier before diffusing away [33]. This competitive effect is discussed mathematically in Section 4.2.2.

The production of some larger molecules than methanol on cold grains via reactions involving atoms and slower molecules has been reported in an earlier review article in this journal [93]. Among the species formed at least partially by sequences of reactions with atomic hydrogen are glycolaldehyde (CH_2OHCHO) and ethylene glycol (($CH_2OH)_2$) (see esp. their Figure 7). Nevertheless, given the large numbers of terrestrial-type organic molecules, listed in Table 3, and found in the gas of warmer regions as well as other sources, additional mechanisms are needed to produce them.

3. Molecular synthesis in subsequent stages of star formation

3.1. Hot core/corino chemistry

As depicted in Figure 1, the formation of both low-mass and high-mass stars occurs through evolutionary stages, one of which is known as a 'hot core' or, for low-mass stars, occasionally as a 'hot corino'. This transitory collapsing stage is warmer than cold cores or infra-red dark cores with typical gas temperatures in the range of 100–300 K. The current leading hypothesis for the chemistry that leads to most of the terrestrial-type species depicted in Table 3 is shown in Figure 3. As the condensation at the center of the collapsing core becomes optically thick, the collapse becomes adiabatic and the central condensation of the core heats up. The outer gas and dust continues to collapse onto the central condensation, and a so-called protostar results. At the same time, changes occur in both the gas-phase and grain-surface chemistry, somewhat akin to the laboratory technique known as temperature-programmed desorption, albeit much slower in the rise of temperature [78]. At temperatures in the vicinity of 30 K, the more vaporisable of the ices in the grain mantles desorb; these species include CO and CH_4. Methane can act as a precursor for a new round of ion-neutral chemistry, known as WCCC (warm carbon-chain chemistry) [94]. Other gas-phase reactions, with small activation energies begin to turn

on as the temperature warms further. Meanwhile, the less vaporisable molecules on and in the grain mantles begin to diffuse and collide with one another. Although most of these molecules are not reactive, they can be activated into energetic radicals by photon, electron, or cosmic ray bombardment . The photons are formed by processes initiated by cosmic ray bombardment of molecular hydrogen [95,96]. Most simulations of the warm-up chemistry, as discussed in Section 5, use photons rather than other particles to produce radicals, and include the assumption that cross-sections for photodissociation are the same as those studied for gas-phase species. The radicals are not destroyed immediately by reaction with hydrogen atoms because these atoms desorb quite quickly from grains warmer than ≈ 15 K, so that association reactions between radicals can take place to produce larger and more saturated species such as alcohols, hydrocarbons, esters, and nitriles [97–100]. For example, bombardment of methanol and formaldehyde ices can lead to the production of the radicals CH_3, CH_3O, CH_2OH, and HCO, which can possibly recombine to form dimethyl ether, methyl formate, and glycolaldehyde.

Experiments in the laboratory show that photon or heavy particle bombardment can indeed lead to the production of these terrestrial-type molecules from mixed ices analogous to interstellar grain mantles, but the frequency of the bombardment far exceeds that in space and the complex chain of reactions that produces these species is not fully understood [101]. Few experiments that study individual association reactions between radicals have been undertaken. Arguments have been made that radical–radical association reactions may not occur facilely on ice mantles and that abstraction reactions might be quite competitive [102]. Experiments also show that some surface reactions can produce complex molecules from ices at low temperatures (≈ 20 K); the production of ethylene glycol and glycolaldehyde appear to be especially efficient if large amounts of the formyl radical (HCO) can be produced from H and CO and the diffusion of HCO over large distances is not needed [92]. Whether or not the products can then desorb into the gas and at what efficiency is unclear. This thermal production is explained in more detail in Section 4.2.2.

In hot cores and hot corinos as well as other warm objects, desorption of molecules from grain mantles occurs primarily thermally rather than via the non-thermal mechanisms needed for low temperature sources. Assuming that the desorption does not occur following a chemical reaction, thermal desorption can be treated as a first-order process and the rate constant k_{TD} is given by Equation (19) [76,78]. At 10 K, thermal desorption is not efficient for any molecular species, although by 15 K, H atoms can begin to desorb. As the temperature nears 30 K, both CO and methane start to desorb, as discussed above. Eventually, as the temperature warms to over 100 K, thermal desorption into the gas begins to take place for the less volatile species, enriching the hot core in terrestrial-type species and eventually totally depleting the ice mantles.

3.2. Protoplanetary discs

As the material continues to collapse past the hot-core stage, further physical effects occur depending on the eventual mass of the star. We focus here on low-mass star formation because it is better understood, and leads to planets. The collapse next leads to objects known as protoplanetary discs, which are cylindrically symmetric objects with a young star or proto-star in the centre. Hydrodynamical calculations are being used to follow the collapse, but at present they cannot be run long enough to produce a mature disc, which
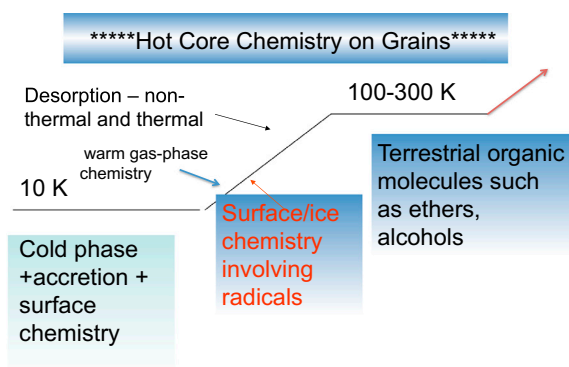
Figure 3. Chemical stages as a cold core warms up to become a hot core. Most of the chemistry is thought to occur on granular ices as warm-up proceeds.

has a lifetime on the order of 10^6 yr. Hydrodynamical calculations have predicted spiral arms in the planes of structures of immature discs [103], and recent observations have shown assorted unusual geometries, including structures leading to binary stars [104]. Semi-empirical collapse models are available and allow much more detailed chemical treatments [105,106].

An artist's rendition of the disc around the star TW Hydrae is shown in Figure 4, based on data from the Herschel Space Telescope. The collapse from the hot core stage to the protoplanetary disc stage is a complex one, and involves violent winds in the North-South direction, which blow away much of the so-called stellar envelope of cool material. These winds contain molecules such as methanol, and the border of the winds and the disc is itself a source of molecules [106]. The disc formed is not perfectly flat, but flares out as distance from the young star increases. Both the physical conditions and the chemistry are strongly heterogeneous. Material in the so-called midplane of the disc drops in density and temperature as a function of distance, while material located both below and above the midplane can be divided into layers in what is known as the 'club sandwich' model [107]. The uppermost and lowermost regions are subjected to radiation from both the interstellar radiation field and the central star itself, while intermediate layers contains gas-phase abundances of a selection of molecules. At the midplane, most of the molecules are found in the dust mantles due to low temperatures (except near the star) and high grain densities. In general, the abundances of gas phase molecules are low compared with other objects, and a relatively complex organic molecule – methanol – has only recently been detected in this disc (and no others) with the ALMA interferometer [108]. This interferometer has also been used under ultra-high spatial resolution to detect a ring pattern, seen in false color in Figure 5. The current interpretation of the black rings involves the assumption that the dust particles in the disc have condensed into larger objects, possibly into planets, which are difficult to see in the submillimeter emission detected by the telescopes, whereas the continuum from individual dust particles has overall a much larger surface area to emit from. Infrared astronomy has been used to detect some hot gaseous molecules in the hot inner regions of discs, including HCN and C_2H_2.
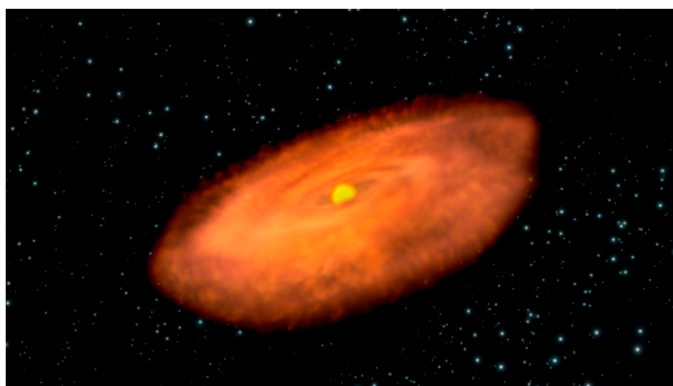
Figure 4. Artist's rendition of a protoplanetary disc around TW Hydrae. Credit: ESA-Christophe Carreau; http://sci.esa.int/herschel/51326-artist-s-impression-of-the-protoplanetary-disc-around-tw-hydrae/.

The chemical processes that occur in protoplanetary discs are quite diverse and include much of what has been discussed so far [109]. It is currently not clear whether chemistry in the disc or molecules formed at earlier stages and swept into the disc dominates. One area of intense current interest is an understanding of what are known as 'snow lines,' which are defined as the minimum distance from a central star at which molecules can remain as ices rather than subliming into the gas. Although the snow line for water is possibly the most important, snow lines for other molecules are also known and are far easier to detect [110]. One reason for the importance of snow lines is that the presence of ice in the solid phase accelerates the agglomeration of dust particles into larger solid entities by softening the collisions between smaller particles.

3.3. Other sources

3.3.1. Photon-dominated regions

In some large dense interstellar clouds, especially those known as 'giant clouds', star formation has already progressed and formed both low-mass and high-mass stars. The latter produce bright hot regions surrounding them known as HII regions, because protons are more abundant than atomic and molecular hydrogen. Farther from the star, the material becomes mainly neutral but is still strongly affected by the intense photon flux from the high-mass star. Such a region is known as a pdr, where the acronym stands for a photon-dominated region, originally known as a photodissociation region [111]. Depending upon the intensity of the radiation field, the temperature can be quite high near the edge of the pdr facing the star. For the bar region of Orion, a peak gas-phase temperature of at least 1000 K is estimated [112], while in the famous Horsehead nebula, also found in Orion but not as strongly excited by an external star, the temperature near the edge is estimated to exceed 100 K [113]. In both cases, the grain temperature is much lower. Under these conditions, if the radiation is sufficiently intense, it is likely that carbon is dominated by the ion C^+, while hydrogen is atomic. Farther from the edge, H is converted into H_2, while C^+ is converted to C, and finally, as the effect of the external radiation is minimised, into CO. The chemistry occurs mainly in the gas phase except in the cold regions of the pdr,

which resemble cold cores. In the Horsehead nebula, the detected molecules can be divided into zones since the nebula is perpendicular to the observer and can be approximated as linear in the direction towards the exciting star. The outermost zone is known as the PAH region, from which PAH emission in the infrared is seen following radiative electronic excitation, and the smaller polyatomic species are not detected except for CCH and C_3H^+. The next zone inwards is known as the PDR zone, while the innermost region is known as the 'Core' [114]. Both carbon-chain and terrestrial-type species are detected in these regions. Detailed gas-grain chemical simulations of the nebula can reproduce many of the observed abundances as a function of depth into the source [113,114].

3.3.2. Shock waves

Shock waves, or shocks for short, are common in the ISM. In the simplest of terms, this complex process is associated with a velocity at which a parcel of high-pressure gas travels into a lower pressure medium; i.e. the ambient cloud, that is stationary except for its thermal motions. The result is a rapid increase in temperature, dependent upon the velocity of the shock and the magnetic field of the medium, which subsequently gradually cools [2]. There are two types of shocks, designated with the letters J and C, which stand for jump and continuous, respectively [115]. In a J shock, the temperature increase is the more rapid and can lead to peak temperatures of 10^4 K before cooling. The highest temperature J shocks can lead to the dissociation of molecules with reformation in the cooling gas. In C-shocks, the magnetic field is large enough to cushion the shock. J-shock chemistry produces some molecules, some of these known as tracers, although these are not large in size. The gaseous molecule SiO can be produced via sputtering of silicate grains in shocked regions such as cloud-cloud collisions [116]. Some shocked outflow sources, the best known of which is L1157, also contain methanol and methyl formate, presumably produced by sputtering after low temperature grain formation [117]. There is strong evidence of general shock sputtering of large molecules into the gas in sources near the center of the Milky Way [118]. Closely related to shock waves is the phenomenon of intermittent turbulence, which has been invoked to explain some chemistry in diffuse clouds that cannot be reproduced by thermal means [119].

4. Recent progress and some remaining uncertainties

In the recent past, a number of new and improved processes have been suggested to explain poorly understood aspects of the chemistry of assorted interstellar sources, mainly the production of complex organic species. Much of this work is still speculative, and awaits more detailed theoretical and experimental treatments. We now consider some of these possibilities, most of which are concerned with cold cores.

4.1. New gas-phase chemistry

4.1.1. Tunnelling and Neutral-neutral radiative association

The recent detection of terrestrial-like molecular species in several cold cores, in particular $HCOOCH_3$ (methyl formate) and CH_3OCH_3 (dimethyl ether), along with previous detections of acetaldehyde (CH_3CHO) and methanol (CH_3OH) suggests that some other mechanism than ion-neutral chemistry is occurring. The production of methanol occurs
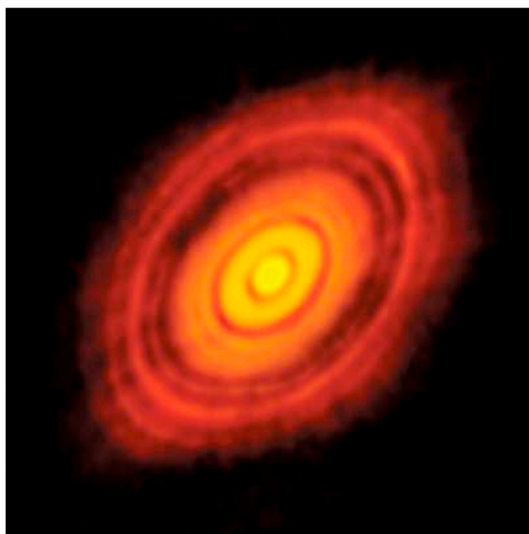
Figure 5. ALMA view of emission from TW Hydrae under high spatial resolution. The object is 175 light years from the earth, and the dark rings are possible orbits of planetary objects. Credit: ALMA ESA/NAOJ/NRAO, C. L. Brogan.

by the hydrogenation of CO on dust mantles, while it is likely that the formation of acetaldehyde occurs via the gas-phase reaction between O and C_2H_5, as shown in Equation (18), as well as surface radical–radical reactions on water ice, although there is some theoretical evidence that the reaction between the radicals CH_3 and HCO cannot occur on amorphous water ice [102]. But the detection of methyl formate and dimethyl ether was indeed a surprise [120], and has elicited a number of solid to speculative suggestions. The work of Balucani et al. [121] reports gas-phase syntheses of both of these species using neutral atoms and molecules, including the fluorine and chlorine atoms. A flow diagram of the syntheses is shown in Figure 6. The syntheses start from methanol, which has been formed on grains and subsequently desorbed non-thermally into the gas phase. Reaction with OH leads rapidly to the methoxy radical at low temperatures:

$$OH + CH_3OH \longrightarrow CH_3O + H_2O \tag{27}$$
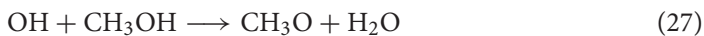
despite the existence of an activation energy barrier [122]. Indeed, the unusual potential surface, which contains an entrance channel complex as well as a barrier, allows tunnelling under the barrier to occur more rapidly at low temperatures due to an increased complex lifetime. The result is a two-order of magnitude enhancement in the rate constant as the temperature drops from 300 to 50 K. Detailed theoretical studies can then be used to obtain the rate constant at a standard cold core temperature of 10 K. Much more work remains to see how general this mechanism is at low temperature and how important such processes can be in chemical simulations. There is also the suggestion that at least some of the low temperature effect comes from the existence of methanol dimers in the apparatus [123].
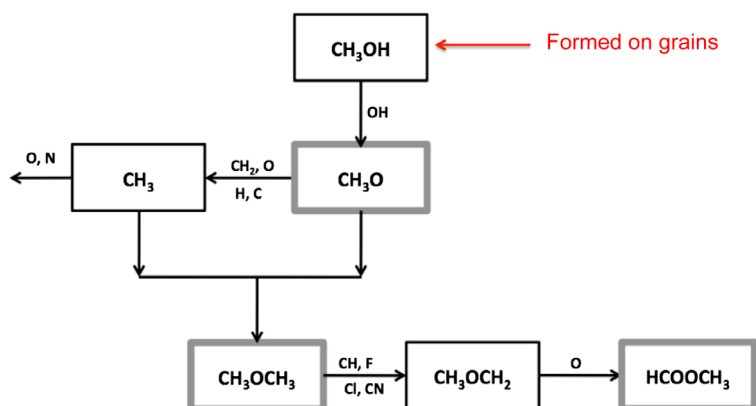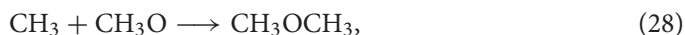
Figure 6. Gas-phase synthesis of dimethyl ether and methyl formate at low temperatures. Taken by permission of Oxford University Press from the article by Balucani et al. in *Monthly Notices of the Royal Astronomical Society*, vol. 449, page L16 (2015).

The methoxy radical can react with a gas-phase methyl radical to produce dimethyl ether:

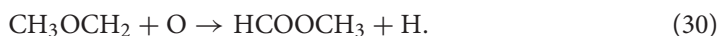$$CH_3 + CH_3O \longrightarrow CH_3OCH_3, \tag{28}$$

by the process of radiative association, as discussed previously in Section 2.1, in which the two reactants form a long-lived complex, which can radiate away enough energy in the form of photons to form the stable product. Although both statistical theories and ion-trap experiments have been utilised to measure or calculate the rate constants of some such reactions that proceed from ion and neutral reactants; e.g. $CH_3^+ + H_2 \longrightarrow CH_5^+$, there is little experimental information concerning neutral–neutral systems [36,37]. Some theoretical treatments, used in conjunction with the chemistry that occurs in the atmosphere of the moon Titan, indicate that neutral–neutral radiative reactions without competitive exothermic channels can occur on every collision if the reactants possess at least three heavy atoms between them [73]. With the assumption that reaction (28) can occur at low temperatures with a rate constant of $\approx 10^{-16} \, \text{m}^3 \, \text{s}^{-1}$, it appears that sufficient dimethyl ether can be produced to explain the observation. Detailed calculations are needed to confirm that the rate constant is indeed this large; an earlier estimate led to a value an order-of-magnitude lower [124].

Dimethyl ether, in this view, is a precursor of methyl formate, which is produced by an abstraction of a hydrogen atom by either a flourine or a chlorine atom:

$$CH_3OCH_3 + F(Cl) \longrightarrow CH_3OCH_2 + HF(HCl), \tag{29}$$

followed by the reaction

$$CH_3OCH_2 + O \rightarrow HCOOCH_3 + H. \tag{30}$$

4.1.2. Proton-transfer reactions

Gas-phase ion-neutral processes are not very efficient in producing terrestrial-like organic species because the final step in the synthesis of such molecules involves dissociative recombination, in which the dominant product channels show sufficient fragmentation that simple two-body channels are most often minor. For example, consider the dissociative recombination of $CH_3OH_2^+$. Experiments show that the production of $CH_3OH + H$ occurs on approximately 3% of reactions [46]. If, instead of reacting with electrons, a protonated ion could competitively react exothermically with a neutral species, the breakup of a heavy atom chain would not likely happen. For example, if protonated ethanol reacts with ammonia, the reaction is likely to be a proton transfer in which the deprotonated neutral species is formed [125]:

$$CH_3CH_2OH_2^+ + NH_3 \longrightarrow CH_3CH_2OH + NH_4^+. \tag{31}$$

Ammonia is indeed unique in undergoing reactions of this type because of its high proton affinity [125]. But for this synthesis to be useful in the ISM, the abundance of ammonia must be quite high. One possibility to obtain such a large gas-phase abundance is for ammonia, which is formed efficiently by the hydrogenation of nitrogen atoms on cold interstellar grains, to desorb non-thermally into the gas phase. This can be achieved by shock waves or by so-called luminosity bursts, which pertain less to cold cores than to protostellar regions [125].

4.2. New surface/ice chemistry

4.2.1. ER and van der Waals mechanisms

Although the inclusion of reactions that proceed via the ER mechanism had been used sparingly if at all in chemical simulations in the past by astrochemists, the search for mechanisms to produce complex molecules at low temperature has led to the utilisation of this mechanism. The rate equation for an ER process is very similar to that for a bimolecular gas-phase reaction. Consider the process

$$A + gr - B \longrightarrow gr - X \tag{32}$$

where 'gr' refers to a species on a grain. The rate for the production of species gr-X is given by the differential equation:

$$\frac{d\theta(X)}{dt} = \sigma_{gr} v_A n(A) \theta(B), \tag{33}$$

where $\theta(X)$ is the probability that a site in the uppermost monolayer is occupied by species X, σ_{gr} is the granular cross section, $n(A)$ is the gaseous concentration of A, and v_A is the perpendicular speed of species A onto the granular surface. The inclusion of the ER mechanism has been reported by Ruaud et al. [82] who emphasised reactions involving atomic carbon as the gas phase species. These reactions must have no activation energy barrier if they are to be important at low temperatures. Assuming that the ER reaction between carbon and an adsorbate X is associative in nature and the product remains on

the grain, we have that

$$C + gr - X \longrightarrow gr - C - X. \qquad (34)$$
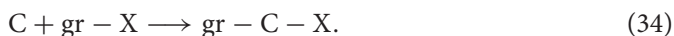
If, however, there is a significant barrier in this step, Ruaud et al. [82] suggested that an alternative mechanism can take place which involves a weakly-bound van der Waals molecule. The process can be written as

$$C + gr - X \longrightarrow gr - C...X, \qquad (35)$$
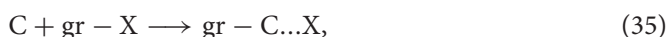
where the three dots signify a weak non-covalent bond. This process likely possesses no activation energy barrier. Once the van der Waals species is formed on the grain surface, the carbon atom can react quickly with mobile atomic hydrogen to form the energised radical gr-CH...X, which can then lead to a variety of products, the most important of which is often thought to be a covalent species designated CHX:

$$gr - C...X + gr - H \longrightarrow gr - CH...X \longrightarrow gr - CHX. \qquad (36)$$
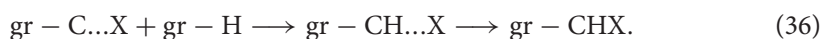
As a specific example of such a mechanism, consider $X = H_2O$. The reaction between C and H_2O possesses an activation energy barrier, so the van der Waals mechanism is invoked, in which the reaction with surface atomic hydrogen leads to two possible radicals: gr-CH_2OH and gr-CH_3O. These products can in turn react associatively with atomic hydrogen to form methanol on the surface. A similar process starting with atomic carbon and gr-methanol leads initially to the van der Waals species gr-C...CH_3OH, which, after reaction with atomic hydrogen to form gr-CH...CH_3OH, leads mainly to the covalent species gr-CH_3OCH_2. Reaction with a second hydrogen atom on the grain then forms dimethyl ether. According to the authors, this mechanism along with non-thermal desorption can form sufficient amounts of the complex molecules CH_3CHO and CH_3OCH_3 in cold cores, but fails to produce enough methyl formate by 2–3 orders of magnitude.

The attempt to find another surface mechanism to produce large molecules efficiently has led some authors to invoke a variant of the hot-atom mechanism. The extra energy needed can be obtained in cold cores via cosmic ray bombardment, which can raise the temperature of whole grains for short periods of time [81], and speed up diffusion. The effect, coupled with possible tunnelling under diffusion barriers, speeds up surface diffusive reactions and enhances the surface production of large molecules according to Reboussin et al. [126]. Nevertheless, it does appear that the mechanism does not produce sufficient abundances to explain the observations of dimethyl ether and methyl formate in cold cores.

4.2.2. Rapid diffusion and competition

The formation of terrestrial-type organic molecules detected in the gas phase in the warm-up to hot cores has been discussed. The principal mechanism is thought to be radical–radical surface reactions at temperatures above 30 K, where radicals can diffuse more easily than at lower temperatures. The radicals are produced by photon bombardment of grains but bombardment by other particles such as electrons and cosmic rays has also been considered. This particular mechanism was thought to be inoperative in cold cores, where radicals cannot diffuse, and also where hydrogen atoms can recombine quickly with any radicals produced. However, recent experiments from the Leiden group at 15 K [92,93,127] show that large terrestrial-type molecules such as glycolaldehyde and ethylene glycol can
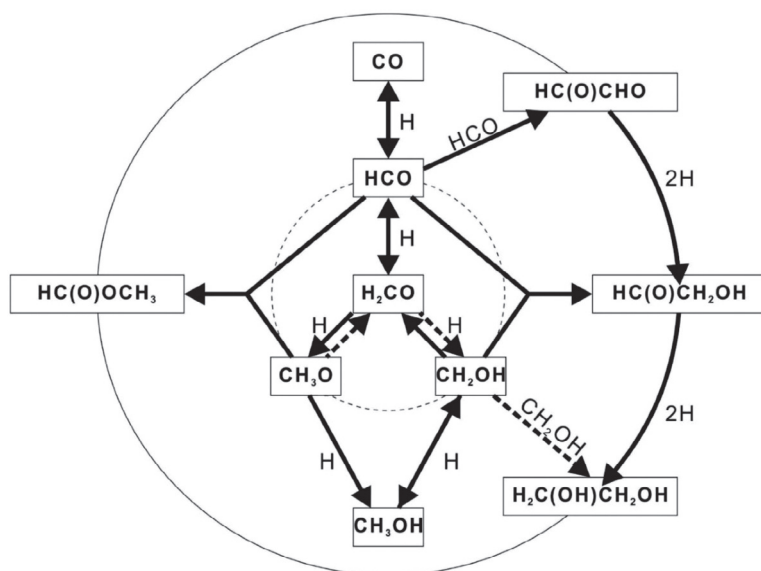
Figure 7. Surface synthesis of glycolaldehyde, ethylene glycol, and possibly methyl formate at low temperatures, as studied by the Leiden group. Taken by permission of Oxford University Press from the article by Chuang et al. in *Monthly Notices of the Royal Astronomical Society*, vol. 455, page 702 (2015).

be produced thermally by surface reactions involving hydrogenation and radical–radical reactions without the need for irradiation. For example, starting from CO ice, reaction with hydrogen atoms leads to the radical HCO. If there are enough of these radicals produced, they can react with each other, leading to a product that upon hydrogenation yields glycolaldehyde and ethylene glycol. The processes are shown in Figure 7, along with a possible synthesis of methyl formate.

To extend the surprising laboratory results for use in interstellar simulations, two modifications involving theoretical diffusion rates have recently been employed, which can enhance the rate of the diffusive surface reaction mechanism at low temperatures so that it can become operative in cold cores, protoplanetary discs, and other cold sources. These two modifications are (i) an increase in the rate of diffusion of surface molecules and (ii) the use of a so-called competitive mechanism [33]. For diffusive reactions without activation energy, the rate of diffusion and hence reaction is enhanced by reducing the barrier against diffusion, E_b, which is expressed as a fraction x of the better studied desorption energy, E_D. Until recently, a value of $x = 0.5$ was used for diffusion on ices composed mainly of water ice [97], but recent treatments can use a reduced value of x of 0.3 or 0.4 [80]. There is some experimental evidence in favour of this reduction [128,129].

The second modification, the competitive mechanism, pertains to surface reactions with a chemical activation energy barrier in addition to the diffusion barriers. If we imagine two species diffusing over a surface, and finding themselves in the same potential well, but facing the additional chemical barrier to reaction, the competition involves diffusion away from the hopping barrier by at least one of the two species vs. reaction via tunnelling through or hopping over the activation energy barrier. Put simply and non-mathematically, if both diffusion barriers for the reactants exceed the activation energy barrier, the reactants can

be trapped in a diffusive well and thus have many chances to tunnel under or hop over the activation energy barrier. Under such circumstances, the rate of reactions with activation energy barriers increases. Mathematically the factor κ discussed in Section 2.3 is changed to [33]

$$\kappa = \frac{k_{\text{tunn}}}{k_{\text{tunn}} + k_{\text{hop,A}} + k_{\text{hop,B}}} \tag{37}$$

where it is assumed that tunnelling under the activation energy barrier dominates hopping over it. The tunnelling rate is given by the equation

$$k_{\text{tunn}} = \nu_0 \times P_{\text{tunn}} \tag{38}$$

where P_{tunn} is the tunnelling probability. In the simplest treatments, the tunnelling is considered to occur through a rectangular barrier, but more realistic potentials have also been utilised [130].

4.2.3. Cosmic-ray bombardment and organic chemistry

The bombardment of the interstellar cloud gas by cosmic rays leads to ion-neutral chemistry, which is an important if not dominant mechanism for the formation of interstellar molecules. In addition, they generate internal photons in dense regions where external electromagnetic radiation cannot penetrate [95,96]. These photons and the photodissociation they cause are critical to the production of radicals on grains in hot core chemical simulations. Besides the interaction of cosmic rays and gas-phase species, especially hydrogen, cosmic rays interact with dust grains in a number of manners. In addition to sputtering and grain heating, the cosmic ray grain penetration can cause chemical effects, in particular involving secondary electrons produced as the rays traverse through the dust particles. A number of experimental investigators have studied the chemical effects of bombarding dust/ice analogues with high energy particles including protons and electrons, as well as utilising the lower energy secondary electrons produced by high-energy particles [131–134]. Although, to the best of our knowledge, only a few attempts have been made to understand the details via theoretical means and simulate their effect in the ISM, it has become clear that granular irradiation is an important mechanism for the formation of organic molecules in the ISM [135].

It is often assumed that the chemistry occurs by radical–radical reactions, just as assumed in the formation of terrestrial-like molecules by photon production of radicals in the warm-up to hot cores. Cosmic ray bombardment of grains, however, can produce secondary electrons to large depths. These electrons can lead to the internal production of both negative and positive ions, the subsequent reactions of which occur at both continuous energies and specific energy quantum mechanical resonances with large cross sections [136]. A detailed treatment to follow this chemistry requires Monte Carlo methods and modern computational approaches. A preliminary Monte Carlo treatment is being developed to mimic the production of ozone ice from oxygen ice in the laboratory [137]. Figure 8 shows a simulation of the path of an incoming 5 keV proton penetrating into a mantle of O_2 ice with the pathways of secondary electrons formed from ionisation events [138].
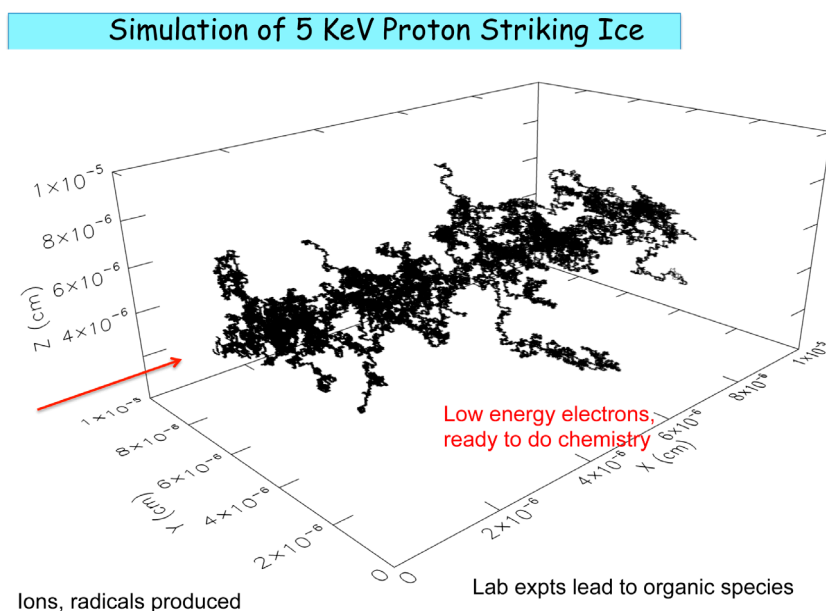
Figure 8. Bombardment of O_2 ice by a 5 KeV proton and the ensuing tracks of secondary electrons.

4.3. Top-down production

In the 1970's, when modern astrochemistry was in its infancy, there was a school of thought that held that interstellar molecules were formed in the cooler portions of high-density stellar atmospheres and, along with bare dust particles, blown out into space to escape, relatively unscathed, to form the initial molecular inventory of interstellar clouds. Although this view has resurfaced [139], the difficulty remains that photodissociation of molecules in unshielded interstellar space takes a short time compared with the time for the journey needed. Exceptions most likely include large molecules such as PAH's, which are relatively immune to rapid photodissociation, at least regarding their skeletal structure. Such species can still dissociate slowly and produce smaller interstellar molecules in diffuse clouds, an example of a mechanism labelled top-down. The view that top-down chemistry involving externally produced precursors is a possibility gained new adherents with the confirmation that the fullerene cation C_{60}^+ is present in diffuse interstellar clouds. The original suggestion that a pair of absorption spectral features in the near infrared belonged to C_{60}^+ had been made based on laboratory evidence in a matrix, not from gas-phase spectroscopy, so was not universally accepted [140]. Only recently was the gas-phase spectrum of this species detected in the laboratory, and it was found that the earlier suggestion concerning its presence in diffuse clouds is correct [7,141,142]. At the time of the original observation, it was suggested that fullerenes could be produced in diffuse and dense interstellar clouds via an ion-neutral mechanism bearing some similarity to the synthesis of carbonaceous species in the laboratory [143]. The interstellar mechanism, however, required a higher density than is present in diffuse clouds, so it was suggested that current diffuse clouds with a measurable abundance of C_{60}^+ had been dense at a previous time and were expanding into the current era. A more popular explanation concerns the formation of fullerenes from

photodissociation of large PAH's, and so is a top-down mechanism. The suggestion is based on the laboratory de-hydrogenation and shrinkage via C_2 units of the PAH $C_{66}H_{20}$ to form neutral C_{60}, and, more generally, appears be active for PAH's with 60–66 carbon atoms, with fewer carbon atoms leading too rapidly to destruction of the PAH and too many carbon atoms leading to structures that cannot show shrinkage via C_2 units [144]. It should be mentioned however, that although the neutral fullerenes C_{60} and C_{70} have been observed in post-stellar structures such as planetary nebulae, the C_{60}^+ cation is the species observed in diffuse clouds.

4.4. Summary of formation mechanisms

In summary, the observation of significant amounts of 'large' terrestrial-type organic species in assorted interstellar sources can now be better explained with the inclusion of recent results in research into chemical simulations, although more theory and experiments are still needed. For cold cores, the abundances of newly detected large molecules can be better explained with (1) new gas-phase reactions involving halogens and radiative association, and (2) granular reactions taking place with more rapid diffusion than assumed in the past along with the inclusion of competition between diffusion and chemical activation barriers, and the use of the ER mechanism for surface reactions in addition to its close cousin – a newly considered mechanism involving weakly-bound van der Waals molecules as intermediates. The existence of large molecules in hot cores can now be explained in part by low-temperature reactions on and in ice mantles as well as cosmic-ray bombardment of these mantles, in addition to the standard theory of photon bombardment to produce reactive radicals in and on mantles. Eventually, the warm-up to hot cores removes the ice mantles containing large molecules from the grains to populate the gas phase. There is even the possibility that some molecules, especially the fullerenes, can be formed in diffuse clouds via photodissociation involving larger PAH's, a top-down mechanism. Classical and newly reported mechanisms contributing to the production of large astronomical molecules in both the gas and on dust particles are listed in Table 4 for the following types of interstellar sources: cold and prestellar cores, the warm-up to hot cores, protoplanetary discs, photon-dominated regions, and diffuse and translucent clouds. Entries in bold face indicate mechanisms assumed to be dominant until more recent work made their stature more ambiguous. For mechanisms that form a unique class of molecules, we use the initials CC for carbon chains and TT for terrestrial-type species.

4.5. Non-thermal desorption

For molecules produced on grains to desorb into the gas where they can be detected by their rotational spectra, either thermal or non-thermal desorption is needed, depending upon the temperature and radiation field. Thermal desorption has already been covered in Section 2.3 so here we discuss only non-thermal mechanisms, which are needed for low-temperature sources. The mechanisms we consider are sputtering and warming of grains by cosmic rays, photodesorption, reactive desorption, and photodissociative desorption. Each of these topics has been studied recently, leading to interesting changes from previous thinking.

Table 4. Possible formation mechanisms for large interstellar molecules.

Source	Gas-phase	Grain/Ice
Cold and pre-stellar cores 10 K	**ion-neutral (CC)** neutral–neutral (CC,TT)	**atom+neutral (TT)** thermal diffusive radical–radical (TT) ER & van der Waals (TT) cosmic ray bombardment
Warm-up to Hot Core/Corino 30–300 K	ion-neutral (CC,TT) neutral–neutral (CC,TT)	**UV-bombardment** **followed by diffusive radical–radical (TT)** cosmic ray bombardment
Protoplanetary Discs Photon-dominated regions 10–1000 K	**ion-neutral (CC)** neutral–neutral (TT) top-down (PAH fragmentation)	**radical–radical (TT)** including chemisorption (CC,TT) cosmic ray bombardment
Diffuse & Translucent Clouds 50–100 K	ion-neutral (CC, fullerenes) (includes dynamics & turbulence) top-down (PAH fragmentation)	cosmic ray bombardment

Notes: (1) bold entries indicate mechanisms previously thought to be dominant in the formation of large organic molecules; (2) TT: terrestrial-type CC: carbon chain (linear, unsaturated).

4.5.1. Sputtering and granular warming by cosmic rays

Cosmic ray bombardment of interstellar grains with ice mantles initiates a rather complex series of events, which can lead to non-thermal desorption via spot heating, whole grain heating, and sputtering. Grain heating increases the rate of thermal desorption depending upon the local or global temperature reached. Since cosmic ray bombardment occurs discretely, the grain temperature does not reach a steady-state value, but rather increases following collision with a cosmic ray and then decreases via desorptive cooling as well as radiative emission. The rate of desorption via global heating depends upon the desorption rate constant as a function of temperature, the energy flux spectrum of the cosmic rays, which consists of the flux of each element, the physics of energy transfer, the diffusion of energy throughout the grain, the peak temperature reached, and the cooling rate. A simple approximation based upon these features [145] yielded the conclusion that grains of radius 0.1 μm within a dense cloud would rapidly reach a temperature of approx. 70 K before cooling. The desorption rate for molecules in ice mantles was calculated as a function of the energy needed for desorption averaged over the cycle of cosmic ray heating and cooling and the long interim between such events. A more recent and more accurate calculation for translucent clouds, in which the external energy flux spectrum of cosmic rays is less reduced than in the interior of dense clouds, obtains a spectrum of temperatures reached following cosmic ray bombardment in the range 20–100 K, with a rate for heating to a maximum temperature of 70 K two orders of magnitude higher than the previous calculation, presumably due mainly to the higher cosmic ray flux in translucent clouds [77]. In addition, the lower maximum temperatures are reached with a much higher frequency, with intervals per grain of only a few years. This calculation has not been incorporated into a determination of the actual rate of desorption because grain cooling has not been included. A calculation involving dense clouds is promised in the near future, which can then be more easily compared with the earlier and simpler approach. Nevertheless, implementation into chemical simulations will require the inclusion of cooling and some averaging. Sputtering occurs via hard collisions involving cosmic rays and grain species. It

can also occur following a sufficiently rapid shock wave [146]. A recent treatment including all of the effects discussed in this section as well as some chemical effects has been reported by Mainitz et al. [147].

4.5.2. Photodesorption

Photodesorption is the process in which a single photon strikes a grain and deposits enough energy to drive an intact molecule into the gas phase. There appear to be a number of distinct mechanisms to power this process, although in some instances it is not clear whether experimentalists have observed intact molecule photodesorption or simply photodissociation. The original experiments involving astrochemical molecules were done within the last decade operating with lamps in what astronomers refer to as the far ultra-violet (FUV), roughly defined as ranging from the Lyman limit (13.6 eV or 91 nm) to approximately 250 nm. Such radiation in interstellar clouds has two sources. First, external stars emit radiation in this region, and astronomers have defined an average radiation field known as the interstellar radiation field (ISRF), which averages and weights contributions from assorted types of stars [3]. This radiation is strongly extinguished by dust particles and photodissociation of abundant molecules such as H_2 in the interior of dense clouds. The second source comes from cosmic rays, which have more penetrating power than FUV photons. In addition to ionisation, cosmic rays produce secondary electrons which excite molecules such as H_2 to emit an internal source of FUV radiation. This second source dominates in dense cloud interiors, although the photon flux is approximately 10^{-4} of the flux of external unshielded radiation [2].

The original laboratory experiments done on astrochemical ices determined an average efficiency of approximately 10^{-3} for desorbed CO molecules per photon coming from the top few monolayers of assorted ices with a hydrogen discharge lamp [148]. The efficiency for N_2 photodesorption was determined to be much less (1.8×10^{-4}), while the efficiency for water ice was determined to be slightly greater than 10^{-3} for thick ices. In addition, OH was detected as well as water, indicating that photodissociation was also occurring [149]. An additional experiment showed that when CO ice was added to N_2 ice, desorption of N_2 was enhanced by a factor of two, presumably by exchange of energy from excited CO molecules [148]. This mechanism is likely similar to a more complex process calculated to be initiated by the resonant absorption of $3.4\,\mu m$ infrared radiation by ice water molecules. The excitation energy is then transferred to the $v = 1$ state of a nearby OH group, which converts a sufficient amount of energy into librational energy of nearby CO molecules to eject them from the ice. The calculated efficiency of desorbed CO molecules per photon was found to be 10^{-4} [150].

Further experiments using tuneable lamps were able to map the efficiency of desorption as a function of wavelength, showing that it mimics to some extent the electronic-vibrational spectrum of the ice. For CO, for example, with its bound A $^1\Pi$ electronic state accessible in the range of the light source, the desorption efficiency as a function of wavelength was found to mimic the electronic spectrum of CO, with an additional width due to the conversion of electronic energy into breaking the desorption bond [151]. For N_2, photodesorption occurs through excitation to the bound b $^1\Pi_u$ state [152]. Yet another experiment, this one using the synchrotron source SOLEIL, showed that the photodesorption seen in a CO:N_2 mixture in which the top two layers consist of a lower CO layer and an upper N_2 layer is indirect in the sense that the layer beneath the top

layer absorbs the photon, but molecules from the top layer are the ones that desorb [153]. For H_2O ice, with continuous absorption to the excited $^1B_1$ electronic state in the range of the tuneable lamp, the efficiency was found to be continuous. A similar continuous photodesorption efficiency was found for methanol.

For molecules such as water and methanol, in which the gas-phase electronic spectrum consists mainly of continuua rather than discrete bands, the photodesorption intensity vs wavelength can be shifted considerably from the gas-phase spectrum, as happens in the case of water. However, for the case of methanol, it is unclear if there is any true photodesorption, because the only products detected are methanol fragments, while the average efficiency of formation of intact gas phase methanol is less than 3×10^{-5} [154]. More experiments are clearly needed, especially for larger molecules.

4.5.3. Reactive desorption

An exothermic surface reaction provides more than enough energy, especially if there is only one product, to drive the physisorbed product off of the grain and into the gas phase. But what is the efficiency of such a process? A simple theoretical treatment based on RRK theory has been developed, in which the exothermicity of reaction can lead statistically to sufficient energy in the surface-product vibrational degree of freedom for desorption of the product [155]. But this rate competes with the rate of product energy loss to the surface. The derived fraction of reaction products that desorb is given by the formula

$$f = \frac{aP}{1 + aP} \tag{39}$$

where P is the RRK probability for the product energy in the surface-product mode to exceed the desorption energy, and a, an empirical parameter, is the ratio of the surface-product mode frequency to the frequency at which energy is lost to the grain surface. The empirical parameter can be fit to molecular dynamics simulations [156] for the case of the surface reaction of H and OH to form water, leading to the result $a = 0.01$. Although it is unclear how general this result is, most astrochemists these days still use this value for a for all reactive desorption processes in their simulations. Since P is typically unity, the calculated efficiency is essentially 0.01 for most reactions.

More recently, experiments have been undertaken and results collected to determine and understand the efficiency of reactive desorption [157,158]. Despite large uncertainties in the results, it was shown that the RRK-based theory is often inadequate, at least for small reactants, and that the efficiency of reactive desorption from bare surfaces such as amorphous silicate and HOPG (highly ordered pyrolitic graphite) tends for some cases to exceed that from amorphous solid water (ASW). For example, the reaction between O and H to form OH at 10 K is measured to have a desorption efficiency of 0.25 on ASW and 0.50 on oxidised HOPG, both values considerably larger than 0.01.

In addition to their experiments, Minnisale et al. [157] found an empirical treatment that fits their experimental results on bare surfaces reasonably well. In their treatment, they assumed that the newly formed product (or products) bounces against the surface elastically with the surface being given an effective mass, and that the energy retained by the product is divided equally among all degrees of freedom. They then used a Boltzmann-type exponential function to compute the probability that the energy of motion in the vertical direction exceeds the desorption energy. For the case of O + H, the approach leads to an

efficiency of desorption of 0.39. If we consider a reaction with more degrees of freedom, such as CO + O, the measured efficiency of desorption at 10 K is given only as an upper limit of 0.10, for both ASW and HOPG. The empirical treatment yields 0.08. In general, the experimental efficiencies for many systems, especially on ASW, are just upper limits, and more work is needed to actually measure them.

Reactive desorption can occur deep inside mantles if the reactants are themselves products of photodissociation, and can recombine, although desorption into the gas is likely to be more difficult than for reactions that occur nearer to the surface.

5. A brief introduction to chemical simulations

Up to now, we have discussed formation pathways concentrating on the larger interstellar molecules, but have offered little proof that these pathways lead to reasonable abundances of these molecules. To calculate the abundances of molecules so as to compare them with abundances obtained from spectroscopic observations through telescopes, it is necessary to develop chemical simulations with large networks of reactions that both form and destroy molecules, both in the gas and on dust particles. By fitting the results of such chemical simulations to observational spectra or abundances for a given source, one can also determine the physical conditions as well as the chemical lifetime of the source. Reaction networks for use in simulations as well as instructions for how to perform simulations can be found on several web sites. One – udfa.net (The UMIST database for astrochemistry) – includes, with few exceptions, only gas-phase reactions while the second – http://kida.obs.u-bordeaux1.fr/a, where 'kida' stands for kinetic database for astrochemistry, lists a variety of gas-phase and gas-grain networks for different types of sources. As an example of their size, the most recent gas-phase network from kida (2014) connects 489 species with 7509 reactions. Some useful general information about networks and codes can be found in a long review article [20]. Many of the reactions in these networks have not been studied in the laboratory or calculated using the techniques of quantum chemistry, especially for the granular reactions. Many have been studied but not over the large temperature range needed for diverse astronomical sources. Sensitivity methods are used to determine which of the unstudied gas-phase reactions should be studied, but this technique is just beginning to be applied to surface processes [20,159].

For each molecule in a network, one can write a kinetic differential equation including all the chemical and physical gain and loss processes. Solutions of these coupled and stiff differential equations can present little difficulty to modern-day computers in many cases. The simplest simulations use time- and spatially-independent physical conditions [160], while more complex simulations can include time-dependent and spatially dependent conditions [105]. The most expensive simulations include chemistry and hydrodynamics to solve problems such as the chemistry that occurs as a dense interstellar cloud is formed from more diffuse gas, or when a protostellar system forms a protoplanetary disc [103,161]. The output is normally in the form of fractional abundances with respect to the total hydrogen density n_H, where $n_H = n(H) + 2n(H_2)$. Uncertainties can be obtained based on the uncertainties in the rate constants of the network utilised [20]. With the inclusion of a radiative transfer code, the output can be put into the form of spectral lines.

For cold regions, where ices build up on interstellar dust grains, a problem arises as to how homogeneously to treat the ice. As mentioned previously, the simplest approach is

known as the two-phase method, in which the phases referred to are the ice mantle and the gas. Here the ice chemistry is assumed to proceed via diffusive surface chemistry but no distinction is made between the outermost monolayer and bulk ice layers. This non-physical approximation can be improved upon by so-called three-phase approaches, in which the ice mantle is divided into an active region consisting of the topmost monolayer or monolayers and a bulk layer. In this case, the chemistry can be restricted to the topmost layer or layers, while the bulk ice remains inert except for photoprocesses [162]. More advanced approaches consider a bulk chemistry and transfer between upper and lower monolayers [80,81,99]. The bulk itself can be divided into individual monolayers although this method is used infrequently [163]. The processes for bulk chemistry include swapping of molecules between different sites as well as processes involving so-called interstitial sites of weak bonding, and those occurring on the internal surfaces of pores in amorphous ices [80,81,99,130,164].

Despite this range of techniques, simulations using rate equations for the solid chemistry can be inaccurate for bare surface and ice mantle chemistry for a number of reasons, including

(1) an inaccurate treatment of random walk for diffusive chemical reactions due to what is known as 'back diffusion.' This problem arises because diffusion can occur in both forward and backward directions, which is not taken care of in the derivation of the expression of the rate constant for diffusion (see equation (20)) unless corrected by more detailed treatments [79],

(2) an overestimate of rate in the so-called 'accretion limit', where the average number of reactive particles for a given species on a grain can be less than unity, and discreteness and fluctuations are critical,

(3) the inability to take account completely of abnormalities in the microscopic structure of the surface, such as roughness, and pores in internal ice layers.

Partial corrections for the second problem have been reported [165,166] and are known as 'modified' rate approaches. These approaches are quite useful. Indeed, the current state-of-the-art for most sources is a three-phase model with modified rates. Problem (3), however, requires a stochastic solution. The first attempts to produce stochastic solutions to granular chemistry utilised probabilistic differential equations, in which solutions are obtained for the probability of a given number of atoms or molecules of a particular species on a grain. This master equation method leads to a formally infinite number of differential equations, which must be terminated artificially [167,168]. Its advantage is that the probabilistic differential equations for surface species and the normal rate equations for the gas-phase species can easily be coupled as a function of time. The termination problem for the surface equations, however, is difficult, and recent approaches use probabilistic equations in place of normal rate equations only when needed. A variant of this technique is the so-called hybrid moment equation method, which has however been used sparingly [169].

It has turned out to be far easier to use macroscopic and microscopic kinetic Monte Carlo approaches. The former are used mainly for gas-phase kinetics [170] (see below). The latter technique, which requires modern computational methods, determines as a function of time the positions of all species in the ice mantle of a single grain. The first generation of such approaches utilised so-called on-lattice methods, in which each species moves

randomly over a lattice of binding sites, depending upon the pseudo-random numbers called [164,171,172]. This method is still used for large reaction networks. More advanced approaches use off-lattice motions, in which pair-wise potentials determine the position of the atoms and molecules on the surface [129,173].

A problem with both Monte Carlo approaches is that if the surface chemistry is treated by such a method, the gas-phase chemistry must also be treated in this manner, because the clock cannot be stochastic for one phase and deterministic for another phase. Another problem is that there is so much hydrogen compared with other molecules that random numbers most often lead to motions of these molecules at the expense of heavier species, greatly increasing the computer time needed. The first problem can be mitigated by using a macroscopic Monte Carlo approach to the gas phase kinetics, so that the positions of the gas-phase species are averaged out and computer time is minimised. The second problem is still unsolved. Because the microscopic Monte Carlo approach yields the position of each atom and molecule in and on a grain mantle, the amount of information obtained is too detailed to be useful, and so must be averaged by starting with different random numbers. A more efficient approach is to use a less detailed Monte Carlo method, in between a macroscopic and totally microscopic approach for the grain chemistry, but these methods have rarely been tried [174]. With a macroscopic method for the gas phase and a microscopic method for the grain mantle, one cannot study easily sources with temperatures above 30–40 K and one cannot run a simulation far beyond 10^5 yr. These two numbers are rather constraining, and most astrochemists today use a three-phase modified rate approach, which can be used both at higher temperatures and for longer periods of time. Nevertheless, the on-lattice macroscopic-microscopic method has been used to study how some large molecules are formed on grains in cold cores [175].

Figure 9 shows one view of the types of simulations of granular chemistry starting from the simplest (bottom right) to the most difficult (top left). The methods at the lowest right portion of the axes are the rate equation approaches without modification, which are the least accurate but can simulate the most complex systems, while next in increasing difficulty as one moves upward and to the left are the modified rate approaches, followed by macroscopic Monte Carlo methods, master equation approaches, on-lattice microscopic Monte Carlo approaches, and finally, the slowest but most accurate, off-lattice microscopic Monte Carlo approaches. Note that, as in the figure, the on-lattice approaches are often referred to as continuous-time random walk (ctrw) and kinetic Monte Carlo (kMC) methods.

6. Conclusions

New observations and chemical analyses have shown that large terrestrial-like classes of organic molecules are observed in a wide assortment of sources in the ISM, most of which are involved in some manner in stellar and planetary formation. These molecules include alcohols, esters, ethers, and nitriles. Most observations have been performed via rotational spectroscopy from spectrometers on the ground or in orbit depending upon the frequencies utilised. Both new gas-phase and grain-surface formation mechanisms have been suggested, with a varying degree of laboratory or theoretical confirmation. Much of the new research has involved the formation of terrestrial-like molecules in cold cores. In the gas, an important role for rapid radiative association reactions between

Methods for grain surface modelling

Microchemical Accuracy

Off-Lattice Monte Carlo

On-Lattice Monte Carlo
(a.k.a CTRW, kMC)

Master equation

Macroscopic Monte-Carlo models

Modified Rate equations

Rate equations
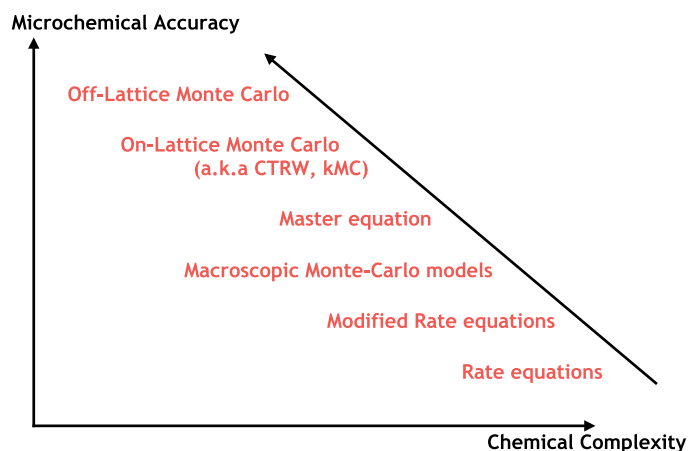
Chemical Complexity

Figure 9. Accuracy vs. chemical complexity for different types of simulations for surface chemistry. Taken with permission from a talk by V. Taquet at the Ice Age Workshop at Lorentz Centre, Leiden University, The Netherlands on 4–8 October 2016.

neutral species has been suggested, although there is no experimental confirmation of such processes, to the best of our knowledge [121]. There is theoretical evidence, although much of this concerns species important in the atmosphere of the Saturnian moon Titan, rather than the ISM [73]. These reactions in addition to neutral–neutral reactions involving halogens lead to the production of the terrestrial-like species methyl formate ($HCOOCH_3$) and dimethyl ether (CH_3OCH_3) in cold sources, in semi-quantitative agreement with observation [121,124]. These and other species such as glycolaldehyde and ethylene glycol can also be produced on and in icy grain mantles via assorted mechanisms, including diffusive (LH) reactions involving a weakly-bound H-atom and a reactive neutral species, ER type reactions involving the formation of a temporary van der Waals intermediate, and radical–radical reactions if a high radical abundance is present or can be formed via photodissociation [82,92]. Surface reactions with activation barriers can occur via enhanced rates due to the competition between tunnelling under such barriers and hopping over diffusion barriers [33,80]. In simple terms, a high diffusion barrier allows the reactants to have many chances to tunnel under a chemical activation energy barrier until diffusion of one or both reactants occurs. Of course, at low temperatures, thermal desorption of heavy species from grain mantles is impossible, so non-thermal desorption must be included in simulations via mechanisms including cosmic ray desorption, photodesorption, reactive desorption, and others discussed in Section 4.5.

At higher temperatures, such as in the formation of hot cores and corinos, many more terrestrial-like large organic molecules are found. The classical mechanism, which has been invoked for the last decade to explain the abundances of these species, relies both on gas-phase chemistry and, more importantly, on radical–radical association reactions on grain surfaces, with radicals produced by photodissociation or other forms of granular irradiation [97–99]. In the early stages of warm-up, the volatile granular species such as methane and acetylene desorb and start a new gas-phase ion-neutral chemistry directed at

larger carbon chain species. At somewhat higher temperatures, heavy radicals can diffuse rapidly enough to form larger terrestrial-type species. At still higher temperatures, thermal desorption allows these less volatile species to be detected in the gas via the sensitive technique of rotational spectroscopy. A suggested enhancement in the importance of ion-neutral chemistry involves the desorption of large abundances of surface ammonia during so-called luminosity outbursts followed by reactions with protonated organic cations, in which the proton is removed from the organic species and added to ammonia, producing the neutral organic molecule [125].

The chemistry that occurs during the conversion of hot cores to protoplanetary discs and once the disc is formed is poorly constrained, partly because the physical changes are complex and have been treated both by three-dimensional hydrodynamics [103,161] and by semi-empirical methods [105,106,176]. The current state of chemical simulations shows that a number of large astronomical molecules in the gas-phase should be detectable in nearby protoplanetary discs by the ALMA telescope, but as of the moment only methanol has been detected in the nearby protoplanetary disc TW Hydrae [108,109].

The reactions that both synthesise and destroy molecules are used with their rate constants in large gas-grain simulations of the chemistry as a function of time [20]. Although many of these reactions have been studied in the laboratory and theoretically, there is still much work to be done in studying other reactions regarded as critical in sensitivity analyses and in extending the temperature range of those already studied. The simulations can be undertaken by approximate methods with kinetic rate equations or, more accurately, with kinetic Monte Carlo approaches. The former can be used over longer periods of time and diverse physical conditions, while the latter are currently constrained to be used at low temperatures for short periods of time, which may not be long enough to determine abundances correctly. It is to be hoped that improvements in the stochastic approach will allow simulations over longer periods of time and under a variety of physical conditions, some of which may be changing in time along with the chemistry.

Disclosure statement

Funding

References

[1] A.G.G.M. Tielens, Rev. Mod. Phys. **85**, 1021 (2013). doi:10.1103/RevModPhys.85.1021.
[2] A.G.G.M. Tielens, *The Physics and Chemistry of the Interstellar Medium* (Cambridge University Press, Cambridge, 2005). doi:10.1017/CBO9780511819056.
[3] D.C.B. Whittet, *Dust in the Galactic Environment*, 2nd ed. (Institute of Physics, Bristol, 2003).
[4] E. Herbst and E.F. van Dishoeck, Ann. Rev. Astron. Astrophys. **47**, 427 (2009). doi:10.1146/annurev-astro-082708-101654.
[5] T. Oka, Chem. Rev. **113**, 8738 (2013). doi:10.1021/cr400266w.
[6] J. Cami, J. Bernard-Salas, E. Peeters, and S.E. Malek, Science **329**, 1180 (2010). doi:10.1126/science.1192035.

[7] G.A.H. Walker, E.K. Campbell, J.P. Maier, D. Bohlender, and L. Malo, Astrophys. J. **831**, 130 (2016). doi:10.3847/0004-637X/831/2/130.

[8] L. Allamandola, A.G.G.M. Tielens, and J.R. Barker, Astrophys. J. Suppl. **71**, 733 (1989). doi:10.1086/191396.

[9] C. Joblin and A.G.G.M. Tielens, editors, *PAHs and the Universe* (EDP Sciences, Les Ulis, 2011).

[10] T.L. Wilson, K. Rohlfs, and S. Huettemeister, *Tools of Radio Astronomy*, 6th ed. (Springer, Heidelberg, 2013).

[11] T.E. Graedel, W.D. Langer, and M.A. Frerking, Astrophys. J. Suppl. **48**, 321 (1982).

[12] K. Acharyya and E. Herbst, Astrophys. J. **812**, 142 (2015). doi:10.1088/0004-637X/812/2/142.

[13] A. Fuente, J. Cernicharo, E. Roueff, M. Gerin, J. Pety, N. Marcelino, R. Bachiller, B. Lefloch, O. Roncero, and A. Aguado, Astron. Astrophys. **593**, A94 (2016). doi:10.1051/0004-6361/201628285.

[14] B.A. McGuire, P.B. Carroll, R.A. Loomis, I.A. Finneran, P.R. Jewell, A.J. Remijan, and G.A. Blake, Science **352**, 1449 (2016). doi:10.1126/science.aae0328.

[15] J.E. Elsila, D.P. Glkavin, J.P. Dworkin, Z. Martins, and J.L. Bada, Proc. Nat. Acad. Sci. US. **109**, E3288 (2012). doi:10.1073/pnas.1213261109.

[16] P. Modica, C. Meinert, P. de Marcelllus, L. Nahon, U.J. Meierhenrich, and L.L. d'Hendecourt, Astrophys. J. **788**, 79 (2014). doi:10.1088/0004-637X/788/1/79.

[17] J.M. Dreiling and T.J. Grey, Phys. Rev. Lett. **113**, 118103 (2014). doi:10.1103/Phys-RevLett.113.118103.

[18] D.C. Lis, G.A. Blake, and E. Herbst, editors, *Astrochemistry: Recent Successes and Current Challenges* (Cambridge University Press, Cambridge, 2006), Section A.

[19] V. Wakelam, J.-C. Loison, E. Herbst, B. Pavone, A. Bergeat, K. Béroff, M. Chabot, A. Faure, D. Galli, W.D. Geppert, D. Gerlich, P. Gratier, N. Harada, K.M. Hickson, P. Honvault, S.J. Klippenstein, S.D. Le Picard, G. Nyman, M. Ruaud, S. Schlemmer, I.R. Sims, D. Talbi, J. Tennyson, and R. Wester, Astrophys. J. Suppl. **217**, 20 (2015). doi:10.1088/0067-0049/217/2/20.

[20] V. Wakelam, I.W.M. Smith, E. Herbst, J. Troe, W. Geppert, H. Linnartz, K. Oberg, E. Roueff, M. Agundez, P. Pernot, H.M. Cuppen, J.-C. Loison, and D. Talbi, Space Sci. Rev. **156**, 13 (2010). doi:10.1007/s11214-010-9712-5.

[21] V.G. Anicich, *An Index of the Literature for Bimolecular Gas Phase Cation-Molecule Reaction Kinetics* (JPL Publication 03-19, NASA, 2003).

[22] A.I. Maergoiz, E.E. Nikitin, and J. Troe, Int. J. Mass Spectrom. **28**, 42 (2009). doi:10.1016/j.ijms.2008.08.019.

[23] T. Su and W.J. Chesnavich, J. Chem. Phys. **76**, 5183 (1982). doi:10.1063/1.442828.

[24] L. Bass, T. Su, W.J. Chesnavich, and M.T. Bowers, Chem. Phys. Lett. **34**, 119 (1975). doi:10.1016/0009-2614(75)80214-4.

[25] K. Ervin, Int. J. Mass Spectrom. **378**, 48 (2015). doi:10.1016/j.ijms.2014.07.009.

[26] W.D. Geppert and M. Larsson, Mol. Phys. **106**, 2199 (2008). doi:10.1080/00268970802322074.

[27] A. Neau, A. Al Khalili, S. Rosen, A. Le Padellec, A.M. Derkatch, W. Shi, L. Vikor, M. Larsson, J. Semaniak, R. Thomas, M.B. Nagard, K. Andersson, H. Danared, and M. af Ugglas, J. Chem. Phys. **113**, 1762 (2000). doi:10.1063/1.481979.

[28] M.J. Jensen, R.C. Bilodeau, C.P. Safvan, K. Seiersen, L.H. Andersen, H.B. Petersen, and O. Heber, Astrophys. J. **543**, 764 (2000). doi:10.1086/apj.2000.543.issue-2.

[29] P.B. Rimmer, E. Herbst, O. Morata, and E. Roueff, Astron. Astrophys. **537**, 7 (2012). doi:10.1051/0004-6361/201117048.

[30] M. Padovani, D. Galli, and A.E. Glassgold, Astron. Astrophys. **501**, 619 (2009), Erratum: **549**, C3 (2013). doi:10.1051/0004-6361/200911794.

[31] N. Indriolo, T.R. Geballe, T. Oka, and B.J. McCall, Astrophys. J. **671**, 1736 (2007). doi:10.1086/523036.

[32] A.J. Markwick (2012). <http://udfa.ajmarkwick.net/index.php?reaction=3921>.

[33] E. Herbst and T.J. Millar, in *Low Temperatures and Cold Molecules*, edited by I.W.M. Smith (Imperial College Press, London, 2008), pp. 1–54.

[34] S. Vissapragada, C.F. Buzard, K.A. Miller, A.P. O'Connor, N. de Ruette, X. Urbain, and D.W. Savin, Astrophys. J. **832**, 31 (2016). doi:10.3847/0004-637X/832/1/31.
[35] D. Gerlich and G. Kaefer, Astrophys. J. **347**, 849 (1989). doi:10.1086/168174.
[36] D. Gerlich and S. Hornung, Chem. Rev. **92**, 1509 (1992). doi:10.1021/cr00015a003.
[37] D.R. Bates, Astrophys. J. **270**, 564 (1983). doi:10.1086/161148.
[38] E. Herbst, Astrophys. J. **237**, 462 (1980). doi:10.1086/157889.
[39] E. Herbst, Astrophys. J. **252**, 810 (1982).
[40] A.A. Maluendes, A.D. McLean, and E. Herbst, Astrophys. J. **417**, 181 (1993). doi:10.1086/173301.
[41] M.B. Mendes, H. Burh, M.H. Berg, M. Froese, M. Grieser, O. Heber, B. Jordon-Thaden, C. Krantz, O. Novotny, S. Novotny, D.A. Orlov, A. Petrignani, M.L. Rappaport, R. Repnow, D. Schwalm, A. Shornikov, J. Stützel, D. Zajfman, and A. Wolf, Astrophys. J. Lett. **746**, L8 (2012). doi:10.1088/2041-8205/746/1/L8.
[42] R.P.A. Bettens and E. Herbst, Astrophys. J. **478**, 585 (1997). doi:10.1086/apj.1997.478.issue-2.
[43] D.J. DeFrees, A.D. McLean, and E. Herbst, Astrophys. J. **293**, 236 (1985). doi:10.1086/163229.
[44] N.G. Adams, D. Smith, K. Giles, and E. Herbst, Astron. Astrophys. **220**, 269 (1985).
[45] A. Luca, D. Voulot, and D. Gerlich, in *WDS02 Proceedings of Contributed Papers, Part, II*, (2002), p. 294.
[46] W.D. Geppert, M. Hamberg, R.D. Thomas, F. Österdahl, F. Hellberg, V. Zhaunerchyk, A. Ehlerding, T.J. Millar, H. Roberts, J. Semaniak, M. AfUgglas, A. Källberg, A. Simonsson, M. Kaminska, and M. Larsson, Faraday Disc. **133**, 177 (2006). doi:10.1039/B516010C.
[47] J. Ramanlal and J. Tennyson, Mon. Not. R. Astron. Soc. **354**, 161 (2004). doi:10.1111/mnr.2004.354.issue-1.
[48] H. Roberts, E. Herbst, and T.J. Millar, Mon. Not. R. Astron. Soc. **336**, 283 (2002). doi:10.1046/j.1365-8711.2002.05738.x.
[49] P. Caselli, C.M. Walmsley, R. Terzieva, and E. Herbst, Astrophys. J. **499**, 234 (1998). doi:10.1086/apj.1998.499.issue-1.
[50] H.T. Roberts, E. Herbst, and T.J. Millar, Astrophys. J. Lett. **591**, L41 (2003). doi:10.1086/376962.
[51] H. Roberts, E. Herbst, and T.J. Millar, Astron. Astrophys. **424**, 905 (2004). doi:10.1051/0004-6361:20040441.
[52] Y. Aikawa, E. Herbst, H. Roberts, and P. Caselli, Astrophys. J. **620**, 330 (2005). doi:10.1086/apj.2005.620.issue-1.
[53] C.N. Shingledecker, J.B. Bergner, R. Le Gal, K.I. Öberg, U. Hincelin, and E. Herbst, Astrophys. J. **830**, 151 (2016). doi:10.3847/0004-637X/830/2/151.
[54] K. Furuya, Y. Aikawa, U. Hincelin, G.E. Hassel, E.A. Bergin, A.I. Vasyunin, and E. Herbst, Astron. Astrophys. **584**, 124 (2015). doi:10.1051/0004-6361/201527050.
[55] L. Pagani, P. Lessafre, M. Jorfi, P. Honvault, T. Gonzalez-Lezana, and A. Faure, Astron. Astrophys. **548**, L4 (2013).
[56] E. Herbst, Astrophys. J. **312**, 351 (1987). doi:10.1086/164880.
[57] E. Wirström, W. Geppert, C. Persson, Å. Hjalmarson, C.M. Perrson, J.H. Black, P. Bergman, T.J. Millar, M. Hamberg, and E. Vigren, Astron. Astrophys. **533**, 24 (2011). doi:10.1051/0004-6361/201116525.
[58] K. Furuya, Y. Aikawa, N. Sakai, and S. Yamamoto, Astrophys. J. **731**, 38 (2011). doi:10.1088/0004-637X/731/1/38.
[59] S.D. Rodgers and S.B. Charnley, Astrophys. J. **689**, 1448 (2008). doi:10.1086/529179.
[60] M. Agundez, J. Cernicharo, M. Guélin, M. Gerin, M.C. McCarthy, and P. Thaddeus, Astron. Astrophys. **4768**, L19 (2008). doi:10.1051/0004-6361:20078985.
[61] C. Walsh, N. Harada, E. Herbst, and T.J. Millar, Astrophys. J. **700**, 752 (2009). doi:10.1088/0004-637X/700/1/752.
[62] M.A. Cordiner and T.J. Millar, Astrophys. J. **697**, 68 (2009). doi:10.1088/0004-637X/697/1/68.
[63] E. Herbst and Y. Osamura, Astrophys. J. **679**, 1670 (2008). doi:10.1086/529159.
[64] N. Douguet, S. Fonseca dos Santos, M. Raoult, O. Dulieu, A.E. Orel, and V. Kokoouline, J. Chem. Phys. **142**, 234309 (2015). doi:10.1063/1.4922691.

[65] F.A. Gianturco, T. Grasse, and R. Wester, J. Phys. B: At., Mol., Opt. Phys. **49**, 204003 (2016). doi:10.1088/0953-4075/49/20/204003.

[66] O. Martinez Jr., Z. Yang, N.J. Demarais, T.P. Snow, and V.M. Bierbaum, Astrophys. J. **720**, 173 (2010). doi:10.1088/0004-637X/720/1/173.

[67] N. Saki, T. Saki, Y. Osamura, and S. Yamamoto, Astrophys. J. **667**, L65 (2007). doi:10.1086/521979.

[68] T.J. Millar, E. Herbst, and R.P.A. Bettens, Mon. Not. R. Astron. Soc. **316**, 195 (2000). doi:10.1046/j.1365-8711.2000.03560.x.

[69] I.W.M. Smith, Angew. Chemie Int. Ed. **45**, 2842 (2006). doi:10.1002/(ISSN)1521-3773.

[70] D. Chastaing, S.D. Le Picard, I.R. Sims, and I.W.M. Smith, Astron. Astrophys. **365**, 241 (2001). doi:10.1051/0004-6361:20000026.

[71] I.R. Sims, J.-L. Queffelec, D. Travers, B.R. Rowe, L.B. Herbert, J. Karthüser, and I.W.M. Smith, Chem. Phys. Lett. **211**, 461 (1993). doi:10.1016/0009-2614(93)87091-G.

[72] D. Chastaing, P.L. James, I.R. Sims, and I.W.M. Smith, Faraday Disc. **109**, 165 (1998). doi:10.1039/a800495a.

[73] V. Vuitton, R.V. Yelle, P. Lavas, and S.J. Klippenstein, Astrophys. J. **744**, 11 (2012). doi:10.1088/0004-637X/744/1/11.

[74] E. Herbst, PCCP **16**, 3344 (2014). doi:10.1039/C3CP54065K.

[75] M.P. Collings and M.R.S. McCoustra, in *European Conference on Laboratory Astrophysics*, edited by C. Stehlé, C. Joblin, and L. d'Hendecourt (EAS Publication Series, 2012), Vol. 58, p. 315.

[76] T.I. Hasegawa, E. Herbst, and C.M. Leung, Astrophys. J. Suppl. **82**, 167 (1992). doi:10.1086/191713.

[77] J. Kalvans, Astrophys. J. Suppl. **224**, 4442 (2016).

[78] K.W. Kolasinski, *Surface Science: Foundations of Catalysis and Nanoscience* (Wiley, Chichester, 2004).

[79] I. Lohmar, J. Krug, and O. Biham, Astron. Astrophys. **504**, L5 (2009). doi:10.1051/0004-6361/200912746.

[80] M. Ruaud, V. Wakelam, and F. Hersant, Mon. Not. Roy. Astron. Soc. **459**, 3756 (2016). doi:10.1093/mnras/stw887.

[81] J. Kalvans, Astrophys. J. **806**, 196 (2015). doi:10.1088/0004-637X/806/2/196.

[82] M. Ruaud, J.C. Loison, K.M. Hickson, P. Gratier, F. Hersant, and V. Wakelam, Mon. Not. Roy. Astron. Soc. **447**, 4004 (2015). doi:10.1093/mnras/stu2709.

[83] M. Minissale, E. Congiu, S. Baouche, H. Chaabouni, A. Moudens, F. Dulieu, M. Accolla, S. Cazaux, G. Manicó, and V. Pirronello, Phys. Rev. Lett. **111**, 053201 (2013). doi:10.1103/PhysRevLett.111.053201.

[84] D. Hollenbach and E.E. Salpeter, Astrophys. J. **163**, 155 (1971). doi:10.1086/150754.

[85] R.J. Gould, and E.E. Salpeter, Astrophys. J. **138**, 393 (1963). doi:10.1086/147654.

[86] J.H. Black, A. Porter, and A. Dalgarno, Astrophys. J. **249**, 138 (1981). doi:10.1086/159269.

[87] N. Katz, I. Furman, O. Biham, V. Pirronello, and G. Vidali, Astrophys. J. **522**, 305 (1999). doi:10.1086/apj.1999.522.issue-1.

[88] S. Cazaux and A.G.G.M. Tielens, Astrophys. J. **604**, 222 (2004); Erratum: Astrophys.J. **715** 698 (2010). doi:10.1088/0004-637X/715/1/698.

[89] E.F. van Dishoeck, E. Herbst, and D.A. Neufeld, Chem. Rev. **113**, 9043 (2013). doi:10.1021/cr4003177.

[90] S.B. Charnley, A.G.G.M. Tielens, and S.D. Rogers, Astrophys. J. **482**, L203 (1997). doi:10.1086/310697.

[91] N. Watanabe and A. Kouchi, Astrophys. J. **571**, L173 (2002). doi: 10.1086/341412.

[92] K.-J. Chuang, G. Fedoseev, S. Ioppolo, E.F. van Dishoeck, and H. Linnartz, Mon. Not. Roy. Astron. Soc. **455**, 1702 (2016). doi: 10.1093/mnras/stv2288.

[93] H. Linnartz, S. Ioppolo, and G. Fedoseev, Int. Rev. Phys. Chem. **34**, 205 (2015). doi: 10.1080/0144235X.2015.1046679.

[94] T. Hirota, N. Saki, and S. Yamamoto, Astrophys. J. **720**, 1370 (2010). Doi: 10.1088/0004-637X/720/2/1370.

[95] S.S. Prasad and S.P. Tarafdar, Astrophys. J. **267**, 603 (1983). doi: 10.1086/160896.
[96] R. Gredel, S. Lepp, A. Dalgarno, and E. Herbst, Astrophys. J. **347**, 289 (1989). doi: 10.1086/168117.
[97] R.T. Garrod, S.L. Widicus Weaver, and E. Herbst, Astrophys. J. **682**, 283 (2008). doi: 10.1086/588035.
[98] J.C. Laas, R.T. Garrod, E. Herbst, and S.L. Widicus Weaver, Astrophys. J. **728**, 71 (2011). doi: 10.1088/0004-637X/728/1/71.
[99] R.T. Garrod, Astrophys. J. **765**, 60 (2013). doi: 10.1088/0004-637X/765/1/60.
[100] R.T. Garrod and S.L. Widicus Weaver, Chem. Rev. **113**, 8939 (2013). doi: 10.1021/cr400147g.
[101] G. Fedoseev, K.-J. Chuang, E.F. van Dishoeck, S. Ioppolo, and H. Linnartz, Mon. Not. Roy. Astron. Soc. **460**, 4297 (2016). doi: 10.1093/mnras/stw1028>
[102] J. Enrique-Romero, A. Rimola, C. Ceccarelli, and N. Balucani, Mon. Not. Roy. Astron. Soc. **459**, l6 (2016). doi: 10.1093/mnrasl/slw031.
[103] H. Yoneda, Y. Tsukamoto, K. Furuya, and Y. Aikawa, Astrophys. J. **833**, 105 (2016).
[104] J.J. Tobin, L.W. Looney, Z.-Y. Li, C. Chandler, M.M. Dunham, D. Segura-Cox, S.I. Sadavoy, C. Melis, R.J. Harris, K. Kratter, and L. Perez, Astrophys. J. **818**, 73 (2016). doi: 10.1093/mnras/stv2288.
[105] M.N. Drozdovskaya, C. Walsh, R. Visser, D. Harsono, and E.F. van Dishoeck, Mon. Not. Roy. Astron. Soc. **445**, 913 (2014). doi: 10.1093/mnras/stu1789.
[106] M.N. Drozdovskaya, C. Walsh, R. Visser, D. Harsono, and E.F. van Dishoeck, Mon. Not. Roy. Astron. Soc. **451**, 3836 (2015). doi: 10.1093/mnras/stv1177.
[107] Y. Aikawa and E. Herbst, Astron. Astrophys. **351**, 233 (1999).
[108] C. Walsh, R.A. Loomis, K.I. Öberg, M. Kama, M.L.R. van't Hoff, T.J. Millar, Y. Aikawa, E. Herbst, S.L. Widicus Weaver, and H. Nomura, Astrophys. J. **823**, L10 (2016).
[109] C. Walsh, T.J. Millar, H. Nomura, E. Herbst, S.L. Widicus Weaver, Y. Aikawa, J.C. Laas, and A.I. Vasyunin, Astron. Astrophys. **563**, 33 (2014). doi: 10.1051/0004-6361/201322446.
[110] C. Qi, P. D'Alessio, K.I. Öberg, D.J. Wilner, A.M. Hughes, S.M. Andrews, and S. Ayala, Astrophys. J. **740**, 84 (2011). doi: 10.1088/0004-637X/740/2/84/.
[111] A.G.G.M. Tielens and D. Hollenbach, Astrophys. J. **291**, 722 (1985). doi:10.1086/163111.
[112] U. Gorti and D.J. Hollenbach, Astrophys. J. **573**, 215 (2002). doi:10.1086/340556.
[113] R.L. Gal, E. Herbst, G. Dufour, P. Gratier, M. Ruaud, and V. Wakelam, in preparation.
[114] V.V. Guzman, J. Pety, P. Gratier, J.R. Goicoechea, M. Gerin, E. Roueff, F. Le Petit, and J. Le Bourlot, Faraday Disc. **168**, 103 (2014).
[115] B.T. Draine, *Physics of the Interstellar and Intergalactic Medium* (Princeton University Press, Princeton, NJ, 2011).
[116] F. Louvet, F. Motte, A. Gusdorf, Q. Nguyên Luong, P. Lesaffre, A. Duarte-Cabral, A. Maury, N. Schneider, T. Hill, P. Schilke, and F. Gueth, Astron. Astrrophys. **595**, 122 (2016). doi:10.1051/0004-6361/201629077.
[117] A.M. Burkhardt, N.M. Dollhopf, J.F. Corby, P.B. Carroll, C.N. Shingledecker, R.A. Loomis, S.T. Booth, G.A. Blake, E. Herbst, A.J. Remijan, and B.A. McGuire, Astrophys. J. **827**, 21 (2016).
[118] E. Mills, M. Morris, R. Güsten, M. Requena Torres, C.C. Lang, N. Butterfield, and J. Ott, BAAS (AAS Meeting 221), 332.06 (2013).
[119] B. Godard, E. Falgarone, and G. Pineau des Forêts, Astron. Astrophys. **570**, 27 (2014). doi:10.1051/0004-6361/201423526.
[120] A. Bacmann, V. Taquet, A. Faure, C. Kahane, and C. Ceccarelli, Astron. Astrophys. **541**, L12 (2012).
[121] N. Balucani, C. Ceccarelli, and V. Taquet, Mon. Not. Roy. Astron. Soc. **449**, 16 (2015). doi:10.1093/mnrasl/slv009.
[122] R.J. Shannon, M.A. Blitz, A.S. Goddard, and D.E. Heard, Nature Chem. **5**, 745 (2013). doi:10.1038/nchem.1692.
[123] W. Siebrand, Z. Smedarchina, E. Martinez-Nunez, and A. Fernandez-Ramos, PCCP. **18**, 22712 (2016). doi:10.1039/c6cp04173f.
[124] A. Vasyunin and E. Herbst, Astrophys. J. **769**, 34 (2013). doi:10.1088/0004-637X/769/1/34.

[125] V. Taquet, E.S. Wirstström, and S.B. Charnley, Astrophys. J. **821**, 46 (2016). doi:10.3847/0004-637X/821/1/46.

[126] L. Reboussin, V. Wakelam, S. Guilloteau, and F. Hersant, Mon. Not. Roy. Astron. Soc. **440**, 3557 (2014). doi:10.1093/mnras/stu462.

[127] G. Fedoseev, H.M. Cuppen, S. Ioppolo, T. Lamberts, and H. Linnartz, Mon. Not. Roy. Astron. Soc. **448**, 3820 (2015). doi:10.1093/mnras/stu2603.

[128] T. Lauck, L. Karssemeijer, K. Shulenberger, M. Rajappan, K.I. Öberg, and H.M. Cuppen, Astrophys. J. **801**, 118 (2015). doi:10.1088/0004-637X/801/2/118.

[129] L.J. Karssemeijer and H.M. Cuppen, Astron. Astrophys. **569**, 107 (2014). doi:10.1051/0004-6361/201424792.

[130] V. Taquet, *Grain surface chemistry in star-forming regions*, Ph. D. thesis, Institut de Planetologie et d'Astrophysique de Grenoble (IPAG), 2012.

[131] M.J. Abplanab and R.I. Kaiser, Astrophys. J. **827**, 132 (2016). doi:10.3847/0004-637X/827/2/132.

[132] M.C. Boyer, N. Rivas, A.A. Tran, C.A. Verish, and C.R. Arumainayagam, Surf. Sci. **652**, 26 (2016).

[133] R.L. Hudson and M.J. Loeffler, Astrophys. J. **773**, 109 (2013). doi:10.1088/0004-637X/773/2/109.

[134] S. Jheeta, S. Ptasinska, B. Sivaraman, and N.J. Mason, Chem. Phys. Lett. **543**, 208 (2012).

[135] M.J. Abplanalp, S. Gozem, A.I. Krylov, C.N. Shingledecker, E. Herbst, and R.I. Kaiser, PNAS **113**, 7727 (2016). doi:10.1073/pnas.1604426113.

[136] C.R. Arumainayagam, H.D. Lee, R.B. Nelson, D.R. Haines, and R. Gunawardane, Surf. Sci. Rep. **65**, 1 (2010).

[137] R.A. Baragiola, C.L. Atteberry, D.A. Bahr, and M.M. Jakas, Nuclear Inst. Methods Phys. Res. B. **157**, 233 (1999).

[138] C.N. Shingledecker and E. Herbst, in preparation.

[139] L.N. Zack and L.M. Ziurys, Astrophys. J. **765**, 112 (2013).

[140] B.H. Foing and P. Ehrenfreund, Nature **369**, 296 (1994). doi:10.1038/369296a0 .

[141] E.K. Campbell, M. Holz, D. Gerlich, and J.P. Maier, Nature **523**, 322 (2015). doi:10.1080/00268976.2015.1018357.

[142] G.A.H. Walker, D.A. Bohlender, J.P. Maier, and E.K. Campbell, Astrophys. J. **812**, L8 (2015). doi:10.1088/2041-8205/812/1/L8

[143] R.P.A. Bettens and E. Herbst, Astrophys. J. **468**, 686 (1996).

[144] J. Zhen, P. Castellanos, D.M. Paardekooper, and H. Linnartz, Astrophys. J. **797**, L30 (2014).

[145] T.I. Hasegawa and E. Herbst, Mon. Not. Roy. Astron. Soc. **261**, 83 (1993).

[146] I. Jimenez-Serra, P.C. Vaselli, J. Martin-Pintado, and T.W. Hartquist, Astron. Astrophys. **482**, 549 (2008).

[147] M. Mainitz, C. Anders, and H.M. Urbassek, Astron. Astrophys. **592**, 35 (2016). doi:10.1051/0004-6361/201628525.

[148] K.I. Öberg, E.F. van Dishoeck, and H. Linnartz, Astron. Astrophys. **496**, 281 (2009). doi:10.1051/0004-6361/200912464.

[149] K.I. Öberg, H. Linnartz, R. Visser, and E.F. van Dishoeck, Astrophys. J. **693**, 1209 (2009). doi:10.1063/1.3582910

[150] F. Dzegilenko and E. Herbst, Astrophys. J. **443**, 81 (1995).

[151] E.C. Fayolle, M. Bertin, C. Romanzin, X. Michaut, K.I. Öberg, H. Linnartz, and J.-H. Fillion, Astrophys. J. **739**, L36 (2011). doi:10.1021/jp201487u.

[152] E.C. Fayolle, M. Bertin, C. Romanzin, H.A.M. Poderoso, L. Philippe, X. Michaut, P. Jdeseck, H. Linnartz, K.I. Öberg, and J.-H. Fillion, Astron. Astrophys. **556**, 122 (2013).

[153] M. Bertin, E.C. Fayolle, C. Ropmanzin, H.A.M. Poderoso, X. Michaut, L. Philippe, P. Jeseck, K.I. Öberg, H. Linnartz, and J.-H. Fillion, Astrophys. J. **7679**, 120 (2013). doi:10.1051/0004-6361/201321533.

[154] G.A. Cruz-Diaz, R. Martin-Domenech, G.M. Muñoz-Diaz, and Y.-J. Chen, Astron. Astrophys. **592**, 68 (2016). doi:10.1051/0004-6361/201526003.

[155] R.T. Garrod, V. Wakelam, and E. Herbst, Astron. Astrophys. **467**, 1103 (2007). doi:10.1051/0004-6361:20066704.

[156] G.J. Kroes and S. Andersson, in *Astrochemistry Throughout the Universe: Recent Successes and Current Challenges (IAU Symposium 231)*, edited by D.C. Lis, G.A. Blake, and E. Herbst (Cambridge University Press, Cambridge, 2006), pp. 427–442. doi:10.1063/1.3582910.

[157] M. Minissale, F. Dulieu, S. Cazaux, and S. Hocuk, Astron. Astrophys. **585**, 24 (2016). doi:10.1051/0004-6361/201525981.

[158] S. Cazaux, M. Minissale, F. Dulieu, and S. Hocuk, Astron. Astrophys. **585**, 55 (2016). doi:10.1021/jp001785y.

[159] H. Cuppen, talk given at a Leiden University workshop entitled *Ice Age: The Era of the James Webb Space Telescope*, 4–7 October 2016.

[160] K. Acharyya and E. Herbst, Astrophys. J. **822**, 105 (2016).

[161] Y. Aikawa, V. Wakelam, F. Hersant, R.T. Garrod, and E. Herbst, Astrophys. J. **760**, 40 (2012). doi:10.1088/0004-637X/760/1/40.

[162] T.I. Hasegawa and E. Herbst, Mon. Not. Roy. Astron. Soc. **263**, 589 (1993). doi:10.1093/mnras/263.3.589.

[163] V. Taquet, C. Ceccarelli, and C. Kahane, Astron. Astrophys. **538**, 42 (2012). doi:10.1051/0004-6361/201117802.

[164] Q. Chang and E. Herbst, Astrophys. J. **787**, 135 (2014). doi:10.1088/0004-637X/787/2/135.

[165] R.T. Garrod, Astron. Astrophys. **491**, 239 (2008). doi:10.1051/0004-6361:200810518.

[166] R.T. Garrod, A.I. Vasyunin, D.A. Semenov, D.S. Wiebe, and Th. Henning, Astrophys. J. **700**, 43 (2009). doi:10.1088/0004-637X/700/1/L43.

[167] T. Stantcheva, V.I. Shematovich, and E. Herbst, Asstron. Astrophys. **391**, 1069 (2002).doi:10.1051/0004-6361:20020838.

[168] T. Stantcheva and E. Herbst, Astron. Astrophys. **423**, 241 (2004). doi:10.1051/0004-6361:20040433.

[169] F. Du and B. Parise, Astron. Astrophys. **530**, 131 (2011). doi:10.1051/0004-6361/201016262.

[170] A.I. Vasyunin, D.A. Semenov, D.S. Wiebe, and Th. Henning, Astrophys. J. **691**, 1459 (2009).

[171] Q. Chang, H.M. Cuppen, and E. Herbst, Astron. Astrophys. **469**, 973 (2007). doi:10.1051/0004-6361:20077423.

[172] H.M. Cuppen and R.T. Garrod, Astron. Astrophys. **529**, 151 (2011). doi:10.1051/0004-6361/201016013.

[173] R.T. Garrod, Astrophys. J. **778**, 158 (2013). doi:10.1088/0004-637X/778/2/158/meta.

[174] A.I. Vasyunin and E. Herbst, Astrophys. J. **762**, 86 (2013). doi:10.1088/0004-637X/762/2/86/meta.

[175] Q. Chang and E. Herbst, Astrophys. J. **819**, 145 (2016). doi:10.3847/0004-637X/819/2/145/meta.

[176] R. Visser and C.P. Dullemond, Astron. Astrophys. **519**, 28 (2010). doi:10.1051/0004-6361/200913604.